A11100 990027

NAT'L INST OF STANDARDS & TECH R.I.C.
A11100990027
/NBS monograph
QC100 .U556 V102-104;106-110;1 C.1 NBS-P

DATE DUE

MAR 14 1978

JUL 9 [illegible]

DEC 1 1978

7-28-83

AUG 12 1991

GAYLORD

PRINTED IN U.S.A.

ureau of Standards
01 Admin. Bldg.
4 19

NBS MONOGRAPH 102

National Bureau of Standards
JUL 28 1972
1204
QC
100
U556

Effects of Finite Lattice Heat Capacity on Spin-Lattice Relaxation

Theory and Numerical Analysis

U.S. DEPARTMENT OF COMMERCE
NATIONAL BUREAU OF STANDARDS

THE NATIONAL BUREAU OF STANDARDS

The National Bureau of Standards[1] provides measurement and technical information services essential to the efficiency and effectiveness of the work of the Nation's scientists and engineers. The Bureau serves also as a focal point in the Federal Government for assuring maximum application of the physical and engineering sciences to the advancement of technology in industry and commerce. To accomplish this mission, the Bureau is organized into three institutes covering broad program areas of research and services:

THE INSTITUTE FOR BASIC STANDARDS . . . provides the central basis within the United States for a complete and consistent system of physical measurements, coordinates that system with the measurement systems of other nations, and furnishes essential services leading to accurate and uniform physical measurements throughout the Nation's scientific community, industry, and commerce. This Institute comprises a series of divisions, each serving a classical subject matter area:

—Applied Mathematics—Electricity—Metrology—Mechanics—Heat—Atomic Physics—Physical Chemistry—Radiation Physics—Laboratory Astrophysics[2]—Radio Standards Laboratory,[2] which includes Radio Standards Physics and Radio Standards Engineering—Office of Standard Reference Data.

THE INSTITUTE FOR MATERIALS RESEARCH . . . conducts materials research and provides associated materials services including mainly reference materials and data on the properties of materials. Beyond its direct interest to the Nation's scientists and engineers, this Institute yields services which are essential to the advancement of technology in industry and commerce. This Institute is organized primarily by technical fields:

—Analytical Chemistry—Metallurgy—Reactor Radiations—Polymers—Inorganic Materials—Cryogenics[2]—Office of Standard Reference Materials.

THE INSTITUTE FOR APPLIED TECHNOLOGY . . . provides technical services to promote the use of available technology and to facilitate technological innovation in industry and government. The principal elements of this Institute are:

—Building Research—Electronic Instrumentation—Technical Analysis—Center for Computer Sciences and Technology—Textile and Apparel Technology Center—Office of Weights and Measures—Office of Engineering Standards Services—Office of Invention and Innovation—Office of Vehicle Systems Research—Clearinghouse for Federal Scientific and Technical Information[3]—Materials Evaluation Laboratory—NBS/GSA Testing Laboratory.

---

[1] Headquarters and Laboratories at Gaithersburg, Maryland, unless otherwise noted; mailing address Washington, D.C. 20234.

[2] Located at Boulder, Colorado 80302.

[3] Located at 5285 Port Royal Road, Springfield, Virginia 22151.

UNITED STATES DEPARTMENT OF COMMERCE
Alexander B. Trowbridge, *Acting Secretary*

NATIONAL BUREAU OF STANDARDS · *A. V. Astin, Director*

Effects of Finite Lattice Heat Capacity on Spin Lattice Relaxation

Theory and Numerical Analysis

Robert L. Peterson

Institute for Basic Standards
National Bureau of Standards
Boulder, Colorado 80302

National Bureau of Standards Monograph 102

Issued August 1, 1967

For sale by the Superintendent of Documents, U.S. Government Printing Office
Washington, D.C. 20402 – Price 25 cents

Contents

Page

1. Introduction 1
2. Theory 2
3. Spin relaxation for tightly coupled vibrational modes 6
4. Spin relaxation for uncoupled vibrational modes 8
5. Spin relaxation to the resonant phonons coupled to a bath 18
6. Discussion and summary 20
7. References 21

Effects of Finite Lattice Heat Capacity on Spin-Lattice Relaxation

Theory and Numerical Analysis

Robert L. Peterson

The transient magnetic behavior of a paramagnetic substance, after an initial disturbance, is considered theoretically for a variety of situations in which the lattice temperature rises as a result of energy flow from the magnetic (electron spin) system. The relaxation mechanisms considered are the direct process, involving interaction between spins and the resonant-phonon modes, and a T^9 Raman process, involving the remaining phonon modes. It is first assumed that the resonant and remaining modes are strongly coupled to each other, and that the helium bath has been removed (helium temperatures are assumed). The resulting transient behavior typically does not differ much from exponential relaxation (the rate increases somewhat during the relaxation), but the difference should be experimentally observable, particularly if the resonance line is inverted initially.

Next, the opposite extreme is considered—that in which the resonant and remaining modes are totally uncoupled; the helium bath is again assumed to have been removed. Two dramatic effects can then occur, depending upon initial conditions. One is the rapid decay to saturation from initial inversion, due to an avalanching creation of resonant phonons by the spins. The second is the pronounced inhibition of the subsequent decay, with the spins remaining near saturation. This decay rate is typically very much slower than the Raman rate, and is due to the flow of the resonant-phonon energy back into the spin system as the spin energy flows into the remaining lattice. Eventually the rate increases to the Raman rate characteristic of the final lattice temperature. Because of inelastic phonon scattering at crystal boundaries, which couples the phonon modes together, this effect of inhibited decay may be difficult to observe.

Finally, we consider the case of spins coupled only to the resonant phonons, which in turn are coupled to a constant temperature bath, whether this be the helium or the remaining modes. Recent phonon avalanche experiments are discussed in this context. It is pointed out that such experiments, performed in the absence of a bath, may provide a reliable measurement of inelastic phonon-boundary scattering.

Key Words: Spin-lattice relaxation, phonon bottleneck, phonon-boundary scattering, spin-phonon interactions.

1. Introduction

It is our purpose in this Monograph to present many additional graphs of the transient magnetic behavior of a paramagnetic system, to supplement a paper published earlier [Peterson, 1965a]. These graphs show the possible behavior of the magnetization of a paramagnet under conditions in which the lattice containing the magnetic moments can heat up as a result of the magnetic relaxation.

We here consider a broader range of parameter values than in the earlier publication in order to demonstrate the types of transient behavior which can occur under various conditions. With two exceptions, the parameter values used do not correspond to specific, known materials. They are chosen, rather, to illustrate what *can* occur in situations which are physically realizable, although in some cases it may indeed be difficult to approximate closely the models used here. In some materials, there will be more relaxation mechanisms operative than we have considered here, some of which may be as important or more important than those which we take into account. For such materials, the results given here will provide an estimate of the influence of those relaxation mechanisms which we have considered.

In addition to considering broader ranges of parameter values, we here make additional application of the theory used in the earlier work [Peterson, 1965a]. We also extend the theory and apply it to situations not considered previously.

The theory used in this Monograph is developed in section 2. In sections 3 and 4, the conventionally used "bath," typically liquid helium, is assumed to have been removed, or otherwise made ineffective. Heat conduction into or through the crystal support is also assumed to be negligible during the relaxation. Ruby, Benoit, and Jeffries [1962] have reported an experiment using adiabatic demagnetization techniques in which these conditions would seem to be satisfied. Thus, by assumption, energy cannot flow out of the lattice subsequent to a disturbance in the system of magnetic moments. It is this absence of an effective bath which allows the interesting, atypical transient behavior of the magnetization which is the main subject of this Monograph.

In sections 3 and 4, the magnetic moments, hereafter called *spins*, constitute one system; the lattice vibrational modes which couple directly to the spins, and called the *resonant modes*, constitute a second system; and the remaining vibrational modes, which couple to the spins via Raman processes, constitute the third system. In section 3 it is assumed that the resonant and remaining vibrational modes are tightly coupled to one another as compared with their coupling to the spins. This is the case whenever it is observed experimentally that the total spin relaxation rate is the simple sum of the two separate relaxation rates. Section 4 treats the opposite extreme: We assume that the resonant modes are completely uncoupled from the remaining vibrational modes. This is realized physically whenever the spin relaxation times are small compared to the characteristic coupling times of the lattice, i.e., the phonon-phonon and phonon-boundary collision times. At helium temperatures, phonon mean-free-paths as limited by phonon-phonon interactions are usually much greater than the dimensions of the sample. The coupling between modes at the temperatures of interest here is therefore indirect, and results from inelastic scattering of the phonons from boundaries [Ziman, 1960; Casimir, 1938]. The effects of "moderate" coupling between the vibrational modes lie between the extreme cases treated in sections 3 and 4, and are readily estimated for various effective phonon-phonon relaxation times.

In section 5 we re-introduce the constant-temperature bath, allowing it to interact with the lattice vibrations. We consider only the direct coupling of the spins to the resonant modes, assuming the coupling of the spins to the remaining modes to be unimportant, often an excellent assumption. Our reason for investigating this situation is that it is the dominant coupling scheme in the recent "phonon avalanche" experiments of Brya and Wagner [1965, 1966] and Shiren [1966]. Although we had predicted such behavior in general terms in our earlier paper [Peterson, 1965a], we did not consider this specific case there, and wish to examine it in some detail here.

Section 6 summarizes the results, and gives some additional discussion. It is pointed out that spin relaxation in the absence of a bath should provide a useful method for studying the effective phonon-phonon interactions, whether these be direct or indirect.

Figure 1 is a block diagram showing the possible combinations of energy flow considered in this paper, and will be referred to in subsequent sections. Most computations were made with the aid of a digital computer. Where analytical reduction was possible, comparison was made to verify the accuracy of the computer results. Where analytical reduction was not possible, the "mesh" size (Δt) was varied to ensure the accuracy of the computer results.

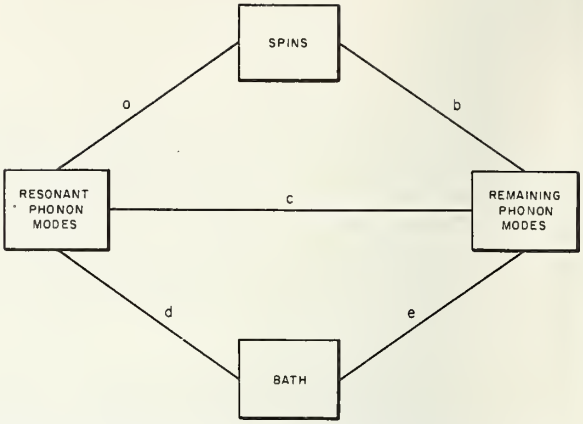

FIGURE 1. *Block diagram of the possible channels of energy flow considered in this Monograph.*

2. Theory

In this section, we develop the theory underlying the rate equations used in subsequent sections, and make an explicit calculation of the relaxation time characterizing the direct process. Because these rate equations are essentially those which are commonly used, except that here all temperatures are allowed to be time-dependent, the reader familiar with these equations may skip this section without impairment to an understanding of the remainder of the paper. Our reason for wanting to develop the underlying theory here is that it does not seem to have been treated carefully elsewhere, except briefly in our earlier paper [Peterson, 1965a]. We also wish to emphasize that a single, unified development can treat a variety of situations, more than just those considered in this paper.

The principal hypothesis is that each system is separately in internal equilibrium, with a well-defined temperature. The temperatures of the various systems are not necessarily equal, and the couplings between the systems bring these temperatures to a common value. It is usually necessary to assume that these couplings are sufficiently weak compared to the interactions internal to the systems, that the temperatures remain well defined while energy flows between the systems. An important exception to this is the two-level system. Another example is discussed later in this section. In these cases the concept of temperature does not need to be introduced, although it may be convenient and intuitively helpful.

The time rate of change of the occupation probabilities of an isolated system, which in our case consists of the *set* of weakly coupled systems, is given approximately by the Pauli master equation, an equation well suited for the study of many relaxation phenomena [Peterson, 1965a and 1965b].

This equation is

$$\frac{d}{dt}\langle\psi|P|\psi\rangle=\sum_{\psi'} W_{\psi\psi'}\ [\langle\psi'|P|\psi'\rangle-\langle\psi|P|\psi\rangle]. \qquad (1)$$

Here $\langle\psi|P|\psi\rangle$ is the probability that the group of systems is in state $|\psi\rangle$, which is an eigenstate of the sum of the Hamiltonians of the individual systems (excluding the coupling between the systems, which constitutes the perturbation V). $W_{\psi\psi'}$ is the transition probability per unit time, which in lowest order is

$$W_{\psi\psi'}=(2\pi/\hbar)|\langle\psi|V|\psi'\rangle|^2\ \delta\{E_\psi-E_{\psi'}\}, \qquad (2)$$

where $\delta\{E_\psi-E_{\psi'}\}$ is the delta function expressing conservation of energy in the group of systems. The state $|\psi\rangle$ for our purposes here may be written as a product of the states [1] of the separate systems:

$$|\psi\rangle\equiv|\alpha_1, \alpha_2, \ldots\rangle=|\alpha_1\rangle|\alpha_2\rangle\ \ldots,$$

where $|\alpha_i\rangle$ is the energy eigenstate for system i, with eigenvalue $E_i(\alpha_i)$.

The average energy of system i at time t is

$$\langle\mathscr{H}_i\rangle_t=\sum_{\alpha_1\alpha_2\ldots} E_i(\alpha_i)\langle\alpha_i\ \ldots|P|\alpha_1, \ldots\rangle=$$

$$=\sum_{\alpha_i} E_i(\alpha_i)\langle\alpha_i|\rho_i|\alpha_i\rangle, \qquad (3)$$

where

$$\langle\alpha_i|\rho_i|\alpha_i\rangle\equiv\sum_{\alpha_1,\alpha_2,\ldots}^{(i)}\langle\alpha_1, \ldots|P|\alpha_1, \ldots\rangle. \qquad (4)$$

The sum in eq (4) excludes system i. $\langle\alpha_i|\rho_i|\alpha_i\rangle$ is just the probability of finding system i in state $|\alpha_i\rangle$. Multiplying eq (1) by $E_i(\alpha_i)$ and summing on all states $|\psi\rangle$, one obtains

$$\frac{d}{dt}\langle\mathscr{H}_i\rangle=\sum_{\psi,\psi'} W_{\psi\psi'}\ [E_i(\alpha_i)$$

$$-E_i(\alpha_i')]\ \langle\psi'|P|\psi'\rangle. \qquad (5)$$

where $|\psi'\rangle\equiv|\alpha_i'\rangle|\alpha_2'\rangle\ \ldots$. The right side of eq (5) is obtained with use of the fact of "microscopic reversibility," $W_{\psi\psi'}=W_{\psi'\psi}$, which follows from eq (2).

The right side of eq (5) is of order V^2. The probability $\langle\psi'|P|\psi'\rangle$ in eq (5) can therefore be factored as

$$\langle\psi'|P|\psi'\rangle=\prod_i\langle\alpha_i|\rho_i|\alpha_i\rangle, \qquad (6)$$

since the correction to eq (6) will be at least of order V, and will not affect the validity of eq (5) to order V^2.

Now V is the sum of the pairwise couplings V_{mn} between all systems. Since V_{mn} contains operators referring only to systems m and n, the matrix elements $\langle\alpha_1, \ldots \alpha_k, \ldots|V_{mn}|\alpha_1', \ldots \alpha_k', \ldots\rangle$ of V_{mn} vanish unless $|\alpha_k\rangle=|\alpha_k'\rangle$ for all k except m and n. Therefore, because of the factor $E_i(\alpha_i)-E_i(\alpha_i')$ on the right in eq (5), the V_{mn} terms in $W_{\psi\psi'}$ cannot contribute unless either $m=i$ or $n=i$. That is, the rate of change of the energy of system i is affected directly only by those systems coupled to system i, which is an intuitive result. The remaining terms in $W_{\psi\psi'}$ are of the form $\langle\psi|V_{im}|\psi'\rangle\langle\psi'|V_{in}|\psi\rangle$. The latter vanish unless $|\alpha_k\rangle=|\alpha_k'\rangle$ for all k except i. The argument of the delta functions multiplying these cross product terms thus reduces to $E_i(\alpha_i)-E_i(\alpha_i')$. But this argument is also the factor appearing in eq (5), and so the cross product terms cannot contribute. Thus eq (5) can be written

$$d\langle\mathscr{H}_i\rangle/dt=\sum_j^{(i)} A_{ij}, \qquad (7)$$

where

$$A_{ij}=\sum_{\psi,\psi'} W(\alpha_i\alpha_i', \alpha_j\alpha_j')\ [E_i(\alpha_i)-E_i(\alpha_i')]$$

$$\prod_{k=1}^{n}\langle\alpha_k'|\rho_k|\alpha_k'\rangle\prod_l{}'\ \delta_{\alpha_l\alpha_l'}, \qquad (8)$$

and

$$W(\alpha_i\alpha_i', \alpha_j\alpha_j')=(2\pi/\hbar)|\langle\alpha_i\alpha_j|V_{ij}|\alpha_i'\alpha_j'\rangle|^2$$

$$\delta\{E_i(\alpha_i)+E_j(\alpha_j)-E_i(\alpha_j')-E_j(\alpha_i')\}. \qquad (9)$$

The product $\prod_l{}'$ in eq (8) excludes systems i and j.

Since

$$\sum_{\alpha_k}\langle\alpha_k|\rho_k|\alpha_k\rangle=1,$$

A_{ij} can be written

$$A_{ij}=\sum_{\alpha_i,\alpha_i'}\sum_{\alpha_j,\alpha_j'} W(\alpha_i\alpha_i', \alpha_j\alpha_j')\ [E_i(\alpha_i)$$

$$-E_i(\alpha_i')]\ \langle\alpha_i'|\rho_i|\alpha_i'\rangle\ \langle\alpha_j'|\rho_j|\alpha_j'\rangle. \qquad (10)$$

Note that eqs (9) and (10) require

$$A_{ij}=-A_{ji}. \qquad (11)$$

Thus, if eq (7) is summed over all systems i, eq (11) shows that the total energy (excluding the weak couplings) is conserved.

In passing from eq (1) to eq (7), no approximations have been made, other than that of eq (5), which does not affect the validity of eq (7) to order V^2, which is the order of eq (1). Now we introduce the hypothesis of thermodynamic equilibrium within each subsystem, with time-dependent temperatures. This idea was apparently first used by Casimir and Du Pre [1938], and has been successfuly applied in many instances since. The left side of eq (7) can then be written

---

[1] This factorization is not possible in the longitudinal spin-spin relaxation problem. See [Peterson, 1965b] and [Philippot, 1964].

$$\frac{d\langle \mathscr{H}_i\rangle}{dt}=\frac{\partial\langle \mathscr{H}_i\rangle}{\partial\beta_i}\frac{d\beta_i}{dt}=-\frac{C_i}{k\beta_i^2}\frac{d\beta_i}{dt} \tag{12}$$

where C_i is the heat capacity of system i, and $\beta_i(t)\equiv[kT_i(t)]^{-1}$, where k is Boltzmann's constant, and $T_i(t)$ is the temperature. In thermal equilibrium, $\langle\alpha_i|\rho_i|\alpha_i\rangle$ will have the form

$$\langle\alpha_i|\rho_i|\alpha_i\rangle=\frac{\exp\left[-\beta_i(t)E_i(\alpha_i)\right]}{\sum\limits_{\alpha_i'}\exp\left[-\beta_i(t)E_i(\alpha_i')\right]}. \tag{13}$$

Substitution of eqs (12) and (13) into (7) then gives a set of coupled first-order, nonlinear differential equations in the variables β_i.

Specializing to a group of three systems, one can write, using eqs (7) and (12),

$$\frac{d\beta_1}{dt}=\frac{\beta_2-\beta_1}{\tau_{12}}+\frac{\beta_3-\beta_1}{\tau_{13}}, \tag{14a}$$

$$\frac{d\beta_2}{dt}=\frac{\beta_1-\beta_2}{\tau_{12}}R_{12}+\frac{\beta_3-\beta_2}{\tau_{23}}, \tag{14b}$$

$$\frac{d\beta_3}{dt}=\frac{\beta_1-\beta_3}{\tau_{13}}R_{13}+\frac{\beta_2-\beta_3}{\tau_{23}}R_{23}, \tag{14c}$$

where

$$\frac{1}{\tau_{ij}}\equiv\frac{k\beta_i^2A_{ij}}{C_i(\beta_i-\beta_j)},\quad R_{ij}\equiv\frac{C_i\beta_j^2}{C_j\beta_i^2}. \tag{15}$$

The "relaxation times" τ_{ij} and ratios R_{ij} of eqs (14) and (15) are of course time dependent, becoming constant asymptotically in time. (A_{ij} becomes proportional to $\beta_i-\beta_j$ in this limit, as may be seen from eq (18) below.) As we have shown earlier [Peterson, 1965b and 1965a], the asymptotic value of τ_{ij}, when system i is a spin system, is the low-temperature generalization of a formula derived by Gorter [1947] and developed further by Hebel and Slichter [Hebel, 1963].

If system i is a spin system s, one may conveniently, and often with negligible loss of accuracy, use a high temperature approximation throughout, as we now show. (If one is interested only in the asymptotic relaxation times of the set of systems, this approximation is readily avoided [Peterson, 1965b].) We assume that the spins, N_s in number, are independent of one another, the usual assumption in spin-lattice relaxation. The spin density matrix can then be factored into a product of density matrices, one for each spin. Further, $W(\alpha_s\alpha_s', \alpha_j\alpha_j')$ decomposes into a sum of transition probabilities, one for each spin, by arguments similar to those preceding eq (7). Taking all spins to be identical, one readily finds that

$$A_{sj}=N_s\sum_{m,m'}\sum_{\alpha_j,\alpha_j'}W(mm',\alpha_j\alpha_j')\,(E_m-E_m')$$

$$\times\langle m'|\rho_s|m'\rangle\,\langle\alpha_j'|\rho_j|\alpha_j'\rangle \tag{16a}$$

$$=\frac{N_s}{2}\sum_{m,m'}\sum_{\alpha_j,\alpha_j'}W(mm',\alpha_j\alpha_j')\,(E_m-E_{m'})$$

$$[\langle m'|\rho_s|m'\rangle\,\langle\alpha_j'|\rho_j|\alpha_j'\rangle-\langle m|\rho_s|m\rangle\,\langle\alpha_j|\rho_j|\alpha_j\rangle], \tag{16b}$$

where E_m is the energy and $\langle m|\rho_s|m\rangle$ is the spin density matrix element of a single spin in state $|m\rangle$, and

$$W(mm',\alpha_j\alpha_j')=(2\pi/\hbar)|\langle m\alpha_j|V_{sj}|m'a_j'\rangle|^2$$

$$\delta\{E_m-E_{m'}+E_j(\alpha_j)-E_j(\alpha_j')\}. \tag{17}$$

Equation (16b) is just the symmetrized form of A_{sj}. Substituting eq (13) into (16b), and noting that $\langle m|\rho_s|m\rangle\,\langle\alpha_j|\rho_j|\alpha_j\rangle$, when multiplied by the energy conserving delta function of eq (17), can be written

$$\langle m'|\rho_s|m'\rangle\,\langle\alpha_j'|\rho_j|\alpha_j'\rangle\ \exp\left[(\beta_j-\beta_s)\,(E_m-E_{m'})\right],$$

one obtains

$$A_{sj}=N_s\sum(E_m-E_{m'})\,[1-\exp(\beta_j-\beta_s)\,(E_m-E_{m'})]$$

$$\langle m'|\rho_s|m'\rangle\,w_j(m',m), \tag{18}$$

where the summation is over all *pairs* of spin states, and

$$w_j(m',m)\equiv\sum_{\alpha_j,\alpha_j'}W(mm',\alpha_j\alpha_j')\,\langle\alpha_j'|\rho_j|\alpha_j'\rangle. \tag{19}$$

[The quantity $w_j(m',m)$ is the transition probability per unit time from state $|m'\rangle$ to state $|m\rangle$, taking into account the influence of system j. By multiplying and dividing the right side of eq (19) by $\langle\alpha_j|\rho_j|\alpha_j\rangle$, and using eqs (13) and (17), one can obtain

$$w_j(m',m)=\sum_{\alpha_j,\alpha_j'}W(mm',\alpha_j\alpha_j')\,\langle\alpha_j|\rho_j|\alpha_j\rangle$$

$$\exp\left[\beta_j(E_{m'}-E_m)\right]$$

$$=w_j(m,m')\exp\left[\beta_j(E_{m'}-E_m)\right], \tag{20}$$

where $w_j(m,m')$ is defined by eq (19) with m and m' interchanged. It is just the transition probability per unit time from $|m\rangle$ to $|m'\rangle$. Equation (20) is the "principal of detailed balance," which ensures that our rate equations are governed by both stimulated and spontaneous processes, as they must be in a proper quantum mechanical treatment.]

The high-temperature approximation, referred to earlier, and often used in spin resonance and relaxation problems, consists of expanding the exponential function of eq (18) and retaining only the term linear in $(\beta_j-\beta_s)$ $(E_{m'}-E_m)$. This quantity is usually much less than unity in magnitude, although for our purposes it is sometimes *initially* about unity. Suppose, for example, that one has initial spin inversion (the worst case from the standpoint of the high-temperature approximation), with $T_j(0)=-T_s(0)=1$ °K. Then

$$|\beta_j-\beta_s)\ (E_{m'}-E_m)|\approx 0.1\ \nu,$$

where ν is in GHz (10^9 cps). At *X*-band ($\nu\approx 10$) this quantity is about unity. As the relaxation progresses, it of course becomes smaller. We show in figure 2 the transient magnetization after initial spin inversion, calculated with and without the high-temperature approximation. A *K*-band level splitting ($\nu\approx 25$, or $\Delta/k\approx 1$ °K) is used, with initial lattice temperatures of 1 °K and 2 °K. Considered in figure 2 is the case of the spins interacting only with the resonant phonons (channels b, c, d, and e in figure 1 are closed). This case is treated in section 5. The high-temperature approximation (equivalent to $\Delta/k=0$) is seen to give a slightly faster spin relaxation rate initially than the equations without this approximation give. The approximation therefore underestimates slightly the delay time before the rapid decay (the "phonon avalanche") characteristic of initial spin inversion, begins. The differences are sufficiently small that one is well justified in using the much simpler high-temperature version of the rate equations for frequencies at *K*-band or lower, and initial lattice temperatures of about 1 °K or higher.

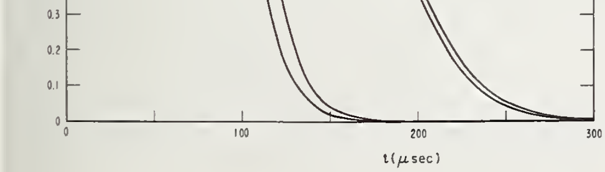

FIGURE 2. *Transient magnetization after initial spin inversion, for two initial lattice temperatures* $T_d(0)$, *as calculated exactly for* K-*band splitting* ($\Delta/k=1$ °K), *and in the high-temperature approximation* ($\Delta/k=0$).
Parameters used are $c_d=10^5$ deg^2 and $a_d=1$ sec^{-1} deg^{-1}. See text for definitions.

There are two other points to consider in the high-temperature approximation. One concerns the spin heat capacity, which contains terms such as $\exp(-\beta_s\Delta)$ where $\Delta=|E_{m'}-E_m|$. For consistency one must write $\exp(-\beta_s\Delta)=1-\beta_s\Delta$. The spin heat capacity is then

$$C_s=\frac{1}{3}S(S+1)N_s\ \Delta^2k\beta_s^2 \tag{21}$$

for N_s independent particles of spin S and energy-level separation Δ. (The concept of a single spin temperature usually is valid only if there is but one pair of spin levels, or if the spin levels are equally spaced. We explicitly consider only the former, using an effective spin of one-half.)

The other point concerns the high-temperature expression for A_{ij} where neither i nor j represents the spin system. Although in this paper we do not have explicit need for such an expression, we point out that the high-temperature approximation may be applied just as with the spin system. The reason is that, in our work, either i or j is always the system of resonant phonon modes, which by definition have energies equal to the energy level splittings in the spin system.

The high-temperature expression for τ_{sj} for a collection of effective spin one-half particles is therefore, by eqs (15), (18), and (21).

$$\tau_{sj}^{-1}=2w_j(m',\ m). \tag{22}$$

Here, $w_j(m',\ m)$ may be used interchangeably with $w_j(mm')$ because of the high-temperature approximations already used. Because system j is a phonon system, and because eq (22) is derived from the lowest-order transition probability expression—which means that only one phonon is created or destroyed when a spin flips—the quantity τ_{sj}^{-1} is the *direct* relaxation rate, hereafter denoted by τ_d^{-1}.

For $w_j(m',\ m)$ given by eq (19), it is well known, and not too difficult to show, that for $E_m-E_{m'}=\Delta>0$, and system j a boson field (phonons or photons),

$$w_j(m',\ m)=A\,\bar{n}_j(\Delta),$$

where A is the Einstein coefficient for spontaneous emission, and $\bar{n}_j(\Delta)$ is the Planck factor, $[e^{\beta_j\Delta}-1]^{-1}$, at temperature $T_j(t)$, giving the number of thermal phonons per mode at energy Δ. The direct relaxation rate is therefore finally given by

$$\tau_d^{-1}=(2Ak/\Delta)T_j(t), \tag{23}$$

in the high-temperature approximation. We remark that this result can be achieved more rapidly by beginning with intuitive rate equations for the spin occupation numbers and phonon occupation numbers. It has been obtained in this way for constant T_j (constant phonon occupation numbers) by many workers. The generalization to a time-dependent resonant-phonon temperature has not been used explicitly in the literature, with the exception of our own earlier work [Peterson, 1965a]. The notion of a steady-state resonant-phonon temperature has been used, however [Van Vleck, 1941; Orbach, 1961; Faughnan and Strandberg, 1961; Scott and Jeffries, 1962]. Actually, the resonant-phonon-temperature language is just an alternate language to that of the phonon occupation numbers, the two concepts being tied together by the Planck factor. The temperature concept is quite convenient to use, as is evidenced by the manner of its appearance in the equations in the following sections, and in many instances is a more intuitively meaningful measure of the degree of phonon excitation than is the phonon number.

The Raman process is a higher-order process, involving any two phonons whose energy difference is equal to that of the spin-flip energy. This process thus makes use of the entire phonon spectrum, with the exception of the resonant phonons. Our use of a single temperature to describe these phonons is now more than a convenient change in language—it is a physical assumption requiring that the phonons interact with one another either directly or indirectly, sufficiently rapidly compared to the spin-phonon interactions that they remain thermalized.

The Raman relaxation rate τ_r^{-1} is considerably more difficult to calculate than τ_d^{-1}, and we shall not derive it here. Orbach's paper [1961] is now the classic for this calculation. Equation (22) is still the basis for the calculation, but the coupling V_{sj} appearing in the transition probability per unit time is replaced by

$$V_{sj}(E_i-\mathscr{H}_{sj})^{-1}V_{sj}, \tag{24}$$

which is the second term in the standard perturbation expansion. $\mathscr{H}_{sj}$ is the sum of the Hamiltonians for the spin and phonon systems, and E_i is the eigenvalue of $\mathscr{H}_{sj}$ in the initial state. V_{sj} is the same operator as in the resonant-phonon case, but now has the effect of bringing in phonons of other than the spin-flip energy. For Kramers' salts, τ_r^{-1} is proportional to the ninth power of the lattice temperature, a result known both experimentally and by calculation (Orbach [1961] lists several earlier references). We do not consider non-Kramers' salts, nor the Orbach two-step process [Orbach, 1961].

In section 5 we consider, among other points, the effects of the phonon-bath interactions, and need the damping time characterizing the rate at which the phonons leak out into the bath. In common with earlier work, we simply adopt the phenomenological notion that the phonon number decays exponentially with a temperature-independent decay time, related to the time of transit of a phonon across the sample.

In the analysis in the subsequent sections, we use numerical values, in the various relaxation time formulas, which have been determined empirically in some cases, or which are representative. The graphs are given in terms of inverse spin-temperature, which is proportional to magnetization in the high-temperature approximation:

$$\langle M_z\rangle=\frac{Tr(e^{-\beta_s\mathscr{H}_s}\;M_z)}{Tr(e^{-\beta_s\mathscr{H}_s})}\approx-\beta_s\frac{Tr_s(\mathscr{H}_sM_z)}{Tr_s(1)}.$$

3. Spin Relaxation for Tightly Coupled Vibrational Modes

In this section, we assume that the resonant modes (designated by *d*, for *direct*) are sufficiently tightly coupled to the remaining vibrational modes (designated by *r*, for *Raman*), that these two systems are effectively a single system with a single lattice temperature $T\equiv(k\beta)^{-1}$. We assume that a constant-temperature bath is not effective. (In fig. 1, channels d and e are closed, and c is "wide open.") In practice, the latter assumption means that the helium is in fact pumped away after the lattice has reached its desired initial temperature, because the spin-lattice times are typically of the order of 0.01 sec to one second, whereas the lattice-bath times are typically much less than a millisecond. Our interest is in discovering the degree of deviation from exponential relaxation caused by the warming-up of the lattice.

By eqs (14b, c), if $\beta_d\equiv\beta_2$ and $\beta_r\equiv\beta_3$ are equal initially, which is the usual experimental situation, then in the limit of small relaxation time τ_{23}, they will remain equal. Equation (14a) then becomes $(1\rightarrow s)$

$$\frac{d\beta_s}{dt}=\frac{\beta-\beta_s}{\tau_1} \tag{25}$$

where

$$\frac{1}{\tau_1}=\frac{1}{\tau_d}+\frac{1}{\tau_r}=a_dT+a_rT^9. \tag{26}$$

The coefficients a_d and a_r refer to the direct and Raman processes, respectively. The T^9 law is characteristic of a Kramers' salt. For the second equation it is convenient to use conservation of energy, which follows from eq (7) as we have pointed out:

$$\frac{C_s}{k\beta_s^2}\frac{d\beta_s}{dt}+\frac{C}{k\beta^2}\frac{d\beta}{dt}=0. \tag{27}$$

Here C is the heat capacity of the entire lattice, given by

$$C=234\,Nk(T/\Theta)^3 \tag{28}$$

in the Debye model for $T\ll\Theta$ ($\Theta=$ Debye temperature). N is the number of lattice sites. In terms of the variables T and $s \equiv k\beta_s = T_s^{-1}$, eqs (25) and (27) are

$$ds/dt = (1 - sT)(a_d + a_r T^8), \tag{25a}$$

and

$$c_r ds/dt = T^3 dT/dt, \tag{27a}$$

where c_r is defined by

$$\frac{\beta^2 C_s}{\beta_s^2 C} \equiv \frac{c_r}{T^5}. \tag{29}$$

By eqs (21) and (28) we have

$$c_r = \frac{1}{4} \frac{N_s}{N} \frac{\Delta^2 \Theta^3}{234 k^2} \tag{30}$$

for $S = \frac{1}{2}$. (The subscript r on c_r is used to make the notation consistent with that of the following sections.)

In figures 3 to 11 is displayed the transient behavior of the inverse spin temperature as given by eqs (25a) and (27a). The curves in figure 3 are based upon parameter values appropriate to the spin concentration and splitting used in a paramagnetic crystal which has been studied extensively [Rannestad and Wagner, 1963; Davids and Wagner, 1964; Baker et al., 1956; Paxman, 1961; Bray et al., 1962]. This is the crystal $K_3Co(CN)_6$ doped with Fe^{3+} ion. For $N_s/N = 10^{-3}$ (Fe/Co $= 1.6\%$), $g = 2.2$, $H = 2000$ Oe (6.2 GHz), and $\Theta = 100$ °K (Θ is not known with certainty [Bray et al., 1962]), one finds $c_r \approx 0.1$ deg^5. The Raman relaxation rate coefficient has the value [Rannestad and Wagner, 1963] $a_r = 0.0043$ sec^{-1} deg^{-9}, and the direct rate coefficient for $H = 2000$ Oe has the value [Davids and Wagner, 1964] $a_d \approx 1$ sec^{-1} deg^{-1}.

Figure 3 is a semilog plot of

$$\frac{s(\infty) - s(t)}{s(\infty)}$$

versus time, for these parameter values and four sets of initial temperatures: $T(0) = -T_s(0) = 2$ °K; $T(0) = -T_s(0) = 1$ °K; $T(0) = 2$ °K, $T_s(0) = \infty$; and $T(0) = 1$ °K, $T_s(0) = \infty$. (The condition $T(0) = -T_s(0)$ is called *complete inversion*, and the condition $T(0) = \infty$ is called *saturation.*) The solid curves give the behavior described by eqs (25a) and (27a); the dashed curves are straight lines, extrapolated back from the asymptotic region (where the relaxation is exponential), to show more clearly the deviation of the solid curves from exponential behavior. It is seen that this deviation is indeed quite small for these parameter values,[2] which correspond to low microwave frequencies, but high spin concentrations. The relaxation is somewhat slower initially than in the asymptotic region. The reason is that the temperature-dependent relaxation rates increase as the lattice temperature slightly rises. From another point of view, one may say that as the spins flip down, the phonon density rises, making the spin transition rates increase.

For the small direct and Raman relaxation rates assumed in figure 3, a helium bath will keep the temperatures of the resonant and remaining phonon modes constant, which undoubtedly is the reason that the two relaxation rates are found, experimentally [Rannestad and Wagner, 1963; Davids and Wagner, 1964; Baker et al., 1956; Paxman, 1961; Bray et al., 1962], to be additive, as we assume in this section. In fact, even if the helium were effectively removed, boundary scattering of the phonons is probably sufficiently inelastic that for the rather long spin times used, the lattice modes are effectively coupled, and would give rise to additive relaxation rates.

In figures 4 and 5, we again use $a_d = 1$ sec^{-1} deg^{-1} and $a_r = 0.0043$ sec^{-1} deg^{-9}, but with c_r increased to 1 deg^5 and 10 deg^5, respectively. (Recall [see eqs (29) and (30)] that an increased value of c_r corresponds to a larger ratio of spin to lattice heat

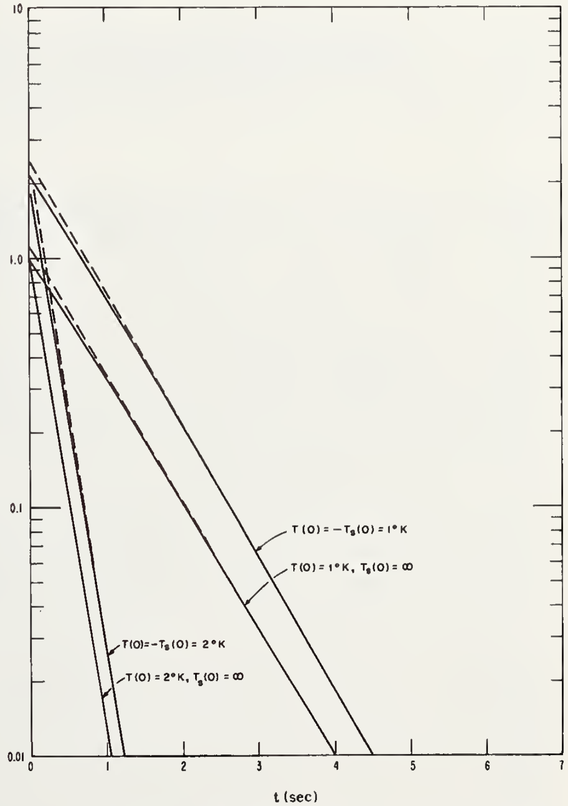

FIGURE 3. *Semi-log plot of transient magnetization after initial saturation and complete inversion.*

Resonant and remaining modes tightly coupled. $a_d = 1$ sec^{-1} deg^{-1}, $a_r = 0.0043$ sec^{-1} deg^{-9}, $c_r = 0.1$ deg^5. The dashed lines are straight lines extrapolated back from the asymptotic regions.

---

[2] The values of c_r used to construct figures 1 and 2 of [Peterson, 1965a] do not correspond to the spin concentration, splitting, and Debye temperatures quoted in the text of that article, due to a numerical error. Figure 3 of the present article is more nearly representative of the $K_3Co(CN)_6$ at 6.2 GHz in the absence of a bath than is figure 2 of [Peterson, 1965a]. The c_r of this article multiplied by k^5 is the same quantity as c in [Peterson, 1965a].

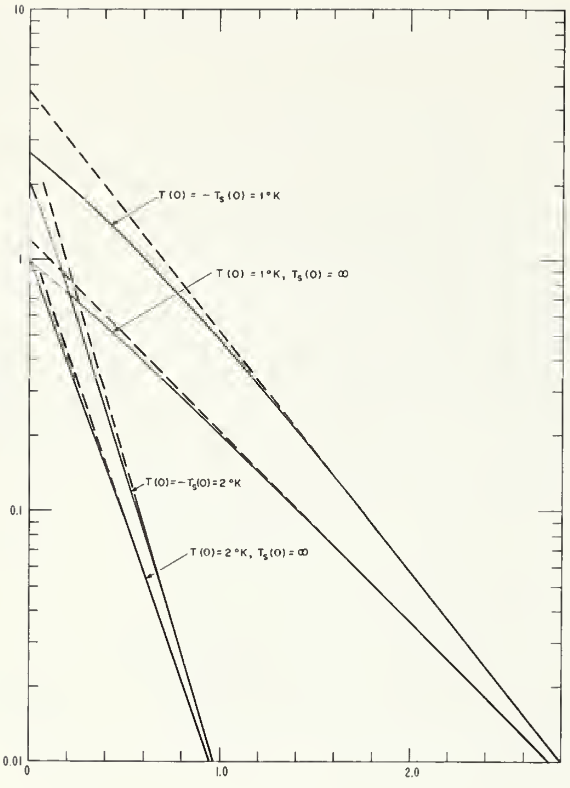

FIGURE 4. *Semi-log plot of transient magnetization after initial saturation and complete inversion.*

Resonant and remaining modes tightly coupled. $a_d=1$ sec^{-1} deg^{-1}, $a_r=0.0043$ sec^{-1} deg^{-9}, $c_r=1$ deg^5. The dashed lines are straight lines extrapolated back from the asymptotic regions.

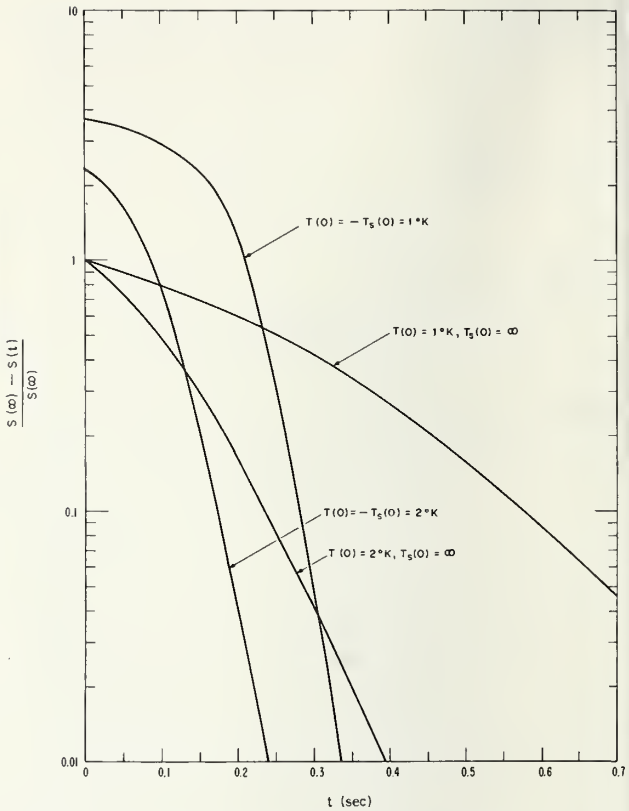

FIGURE 5. *Semi-log plot of transient magnetization after initial saturation and complete inversion.*

Resonant and remaining modes tightly coupled. $a_d=1$ sec^{-1} deg^{-1}, $a_r=0.0043$ sec^{-1} deg^{-9}, $c_r=10$ deg^5.

capacities. An increased value of c_r can result from an increase in spin concentration, a higher Debye temperature, or a larger energy level splitting. The latter can be accomplished by increasing the magnetic field, or sometimes by re-orienting the crystal in the magnetic field.) Deviations from exponential recovery are now quite pronounced. Notice that increased values of c_r shorten the decay times, meaning that the likelihood of observing the nonexponential behavior is enhanced due to better competition of these relaxation mechanisms with any not explicitly included here.

If c_r is increased by means of increasing the magnetic field, then the direct rate will also be increased, going approximately as H^4 for Kramers' salts [Scott and Jeffries, 1962; Orbach, 1961; Kronig, 1939; Van Vleck, 1940]. We have used $a_d=10$ sec^{-1} deg^{-1} and $a_r=0.0043$ sec^{-1} deg^{-9}, with $c_r=1$ deg^5 in figure 6 and $c_r=10$ deg^5 in figure 7, to investigate this effect quantitatively. The deviation from exponential behavior is now decreased from that in figures 4 and 5. The reason is that the direct process now tends to "short circuit" the Raman process. The amount of *change* of the total relaxation rate, due to the increased temperature of the lattice, is thereby decreased. Notice also that the decay times are shortened over those in figures 4 and 5.

In figures 8–11, we have assumed an increased Raman rate, using $a_r=0.01$ and 0.02 sec^{-1} deg^{-9}, with $a_d=1$ and 10 sec^{-1} deg^{-1} and $c_r=1$ and 10 deg^5. The nonexponential characteristics are now more pronounced than in the corresponding figures 4 to 7, and on a still shorter time scale.

We remark that figures 3 to 11 are applicable to a much wider range of relaxation rates than is explicitly indicated. That is, if τ_1 in eq (26) is multiplied by a dimensionless constant f, the only effect is to multiply the times scales of figures 3 to 11 by f. The shapes of the curves do not change.

To sum up this section, we have exhibited in figures 3 to 11, for a rather large range of parameter values, the degree to which the spin relaxation rate increases when the lattice temperature, assumed to characterize the entire phonon spectrum, increases during the relaxation.

4. Spin Relaxation for Uncoupled Vibrational Modes

In this section, we investigate some of the relaxation characteristics of a spin system coupled to the resonant modes via the direct process, and to the remaining vibrational modes via a Raman T^9

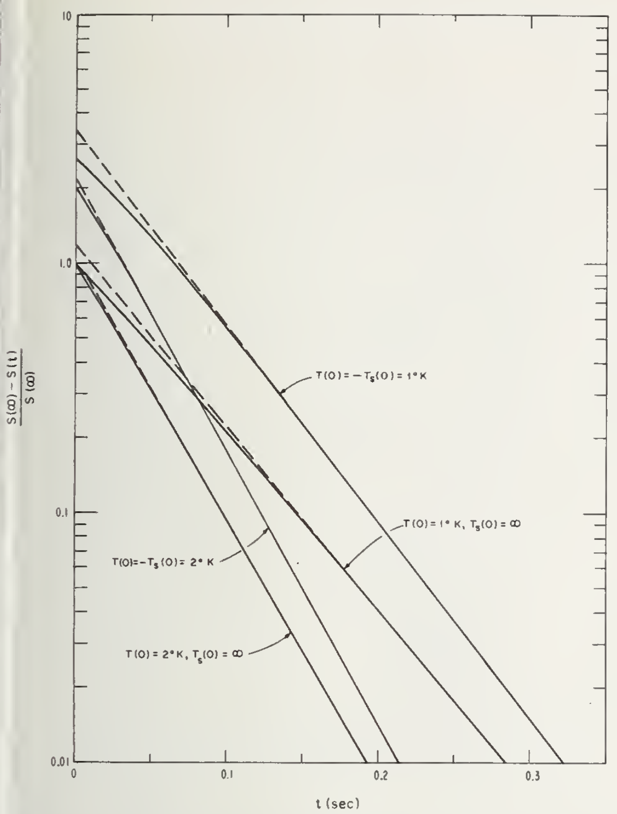

FIGURE 6. *Semi-log plot of transient magnetization after initial saturation and complete inversion.*

Resonant and remaining modes tightly coupled. $a_d=10$ sec^{-1} deg^{-1}, $a_r=0.0043$ sec^{-1} deg^{-1}, $c_r=1$ deg^{-5}. The dashed lines are straight lines extrapolated back from the asymptotic regions.

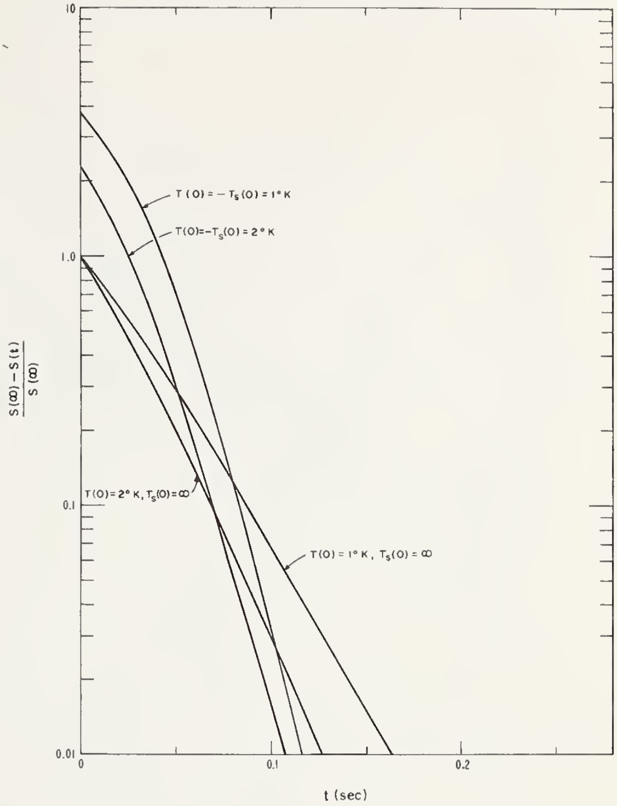

FIGURE 7. *Semi-log plot of transient magnetization after initial saturation and complete inversion.*

Resonant and remaining modes tightly coupled. $a_d=10$ sec^{-1} deg^{-1}, $a_r=0.0043$ sec^{-1} deg^{-1}, $c_r=10$ deg^{-5}.

process, but for which the resonant modes are totally uncoupled to the remaing modes.

In eqs (14), we set τ_{23}^{-1} equal to zero to indicate the lack of coupling between systems $2\equiv d$ and $3\equiv r$. (In fig. 1, channels c, d, and e are closed.) Equations (14) then become

$$\frac{d\beta_s}{dt}=\frac{\beta_d-\beta_s}{\tau_d}+\frac{\beta_r-\beta_s}{\tau_r}. \qquad (31a)$$

$$\frac{d\beta_d}{dt}=\frac{\beta_d-\beta_d}{\tau_d}R_{sd}, \qquad (31b)$$

$$\frac{d\beta_r}{dt}=\frac{\beta_s-\beta_r}{\tau_r}R_{sr}, \qquad (31c)$$

where

$$\tau_d^{-1}=a_dT_d, \qquad \tau_r^{-1}=a_rT_r^9, \qquad (32)$$

and

$$R_{sd}=\frac{C_s\beta_d^2}{C_d\beta_s^2}, \qquad R_{sr}=\frac{C_s\beta_r^2}{C_r\beta_s^2}. \qquad (33)$$

The heat capacity, C_d, of the resonant modes can be written

$$C_d=k\rho(\omega)\delta\omega=9N\Delta^2\hbar\delta\omega/(k^2\Theta^3). \qquad (34)$$

The first equality in eq (34) results because the resonant modes are at the low-frequency end of the lattice vibrational spectrum, so that a heat capacity per mode equal to Boltzmann's constant (the high-temperature expression) can be used. The Debye formula for the density of modes, $\rho(\omega)$, is used in the second equality. Also, $\delta\omega$ is a measure of the bandwidth of modes resonant with the spins, and N is the number of lattice sites.

Setting $s=k\beta_s$, as before, and using T_d and T_r as variables in place of β_d and β_r, one can write eqs (31a, b, c) as

$$ds/dt=a_d(1-sT_d)+a_r(1-sT_r)T_r^8, \qquad (35a)$$

$$dT_d/dt=a_dc_d(1-sT_d), \qquad (35b)$$

$$dT_r/dt=a_rc_r(1-sT_r)T_r^5. \qquad (35c)$$

Here c_r is the same as that of the preceding section, defined by eq (29) and given in eq (30) for $S=\frac{1}{2}$.

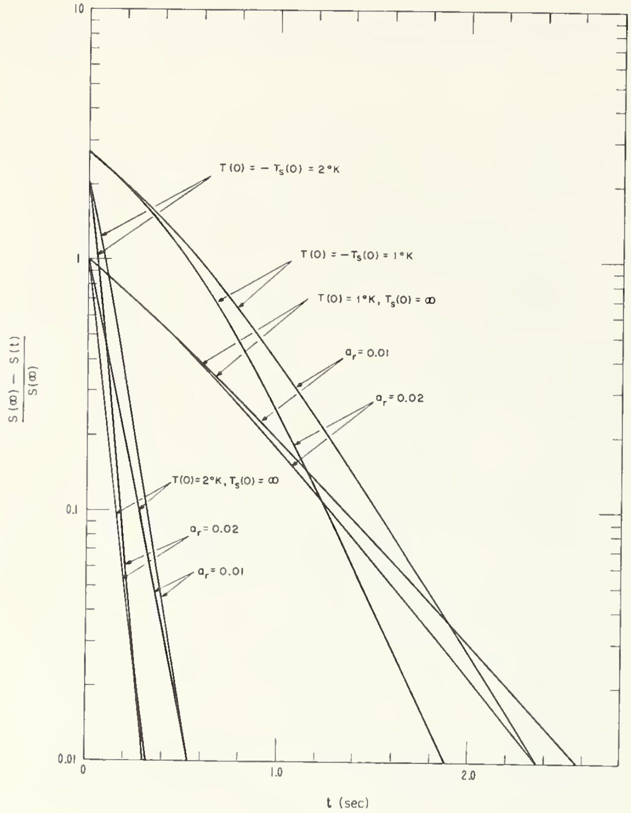

FIGURE 8. *Semi-log plot of transient magnetization after initial saturation and complete inversion.*

Resonant and remaining modes tightly coupled. $a_d = 1$ sec^{-1} deg^{-1}, $a_r = 0.01$ and 0.02 sec^{-1} deg^{-9}, $c_r = 1$ deg^5.

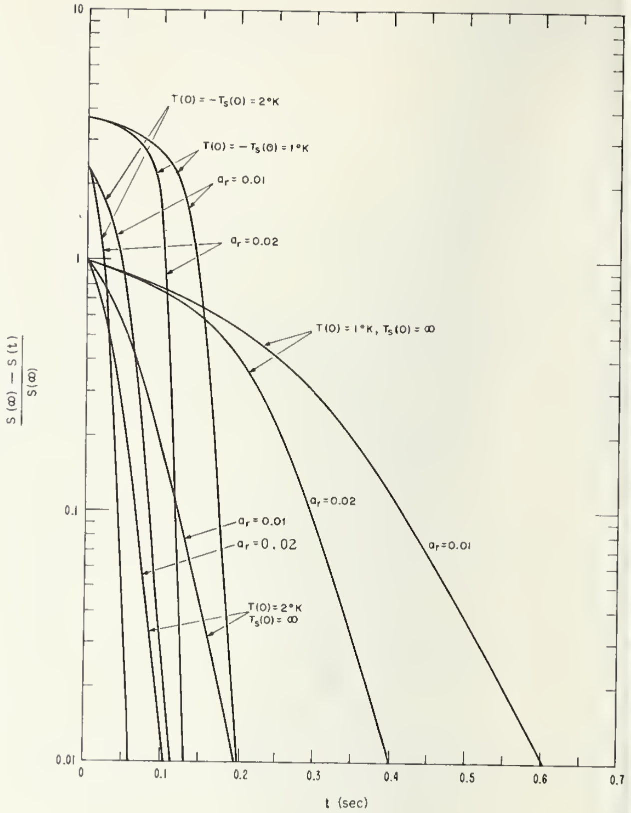

FIGURE 9. *Semi-log plot of transient magnetization after initial saturation and complete inversion.*

Resonant and remaining modes tightly coupled. $a_d = 1$ sec^{-1} deg^{-1}, $a_r = 0.01$ and 0.02 sec^{-1} deg^{-9}, $c_r = 10$ deg^5.

The quantity c_d is defined by

$$R_{sd} = \frac{C_s \beta_d^2}{C_d \beta_s^2} \equiv \frac{c_d}{T_d^2}. \tag{36}$$

Combining eqs (21), (34), and (36), one finds

$$c_d = \frac{N_s}{N} \frac{k\Theta^3}{36\hbar\delta\omega}. \tag{37}$$

Notice that c_d is independent of the level separation Δ, whereas c_r varies as Δ^2. For the values $N_s/N = 10^{-3}$, $\Theta = 100$ °K, and a bandwidth $\delta\omega$ equal to a spin resonance linewidth of $\delta H = 2$ Oe (i.e., $\hbar\delta\omega = g\beta_0\delta H$, where $\beta_0 =$ Bohr magneton), one finds that $c_d \approx 10^5$ deg^2.

One can predict readily the general features of the spin relaxation from consideration of the relative heat capacities and relaxation rates, as well as from consideration of eqs (35). Initially the resonant and remaining modes are at the temperature, say T_0. If the direct and Raman rates are comparable at first, the temperature of the resonant mode system will rise much more rapidly than that of the remaining lattice because of its much smaller heat capacity. Because the spin heat capacity is initially typically much larger than that of the resonant modes, the temperature of the latter will rise very high. A qualitative difference in the spin relaxation occurs, according to whether the spin system is initially saturated or inverted. For initial saturation ($s_0 = 0$) eqs (35) give

$$\frac{ds_0}{dt}\,(\text{saturation}) = \frac{1}{T_0}\left(\frac{1}{\tau_{d0}} + \frac{1}{\tau_{r0}}\right), \tag{38a}$$

$$\frac{d^2 s_0}{dt^2}\,(\text{saturation}) = \frac{-1}{T_0}\left[\left(\frac{1}{\tau_{d0}} + \frac{1}{\tau_{r0}}\right)^2 - \frac{8c_r}{T_0^5 \tau_{r0}^2}\right], \tag{38b}$$

where the subscript zeroes refer to the initial time. The initial curvature $(d^2 s_0/dt^2)$ is typically negative. For initial complete inversion, eqs (35) give

$$\frac{ds_0}{dt}\,(\text{inversion}) = \frac{2ds_0}{dt}\,(\text{saturation}), \tag{38c}$$

$$\frac{d^2 s_0}{dt^2}\,(\text{inversion}) \approx \frac{2c_d}{T_0^3 \tau_{d0}^2}. \tag{38d}$$

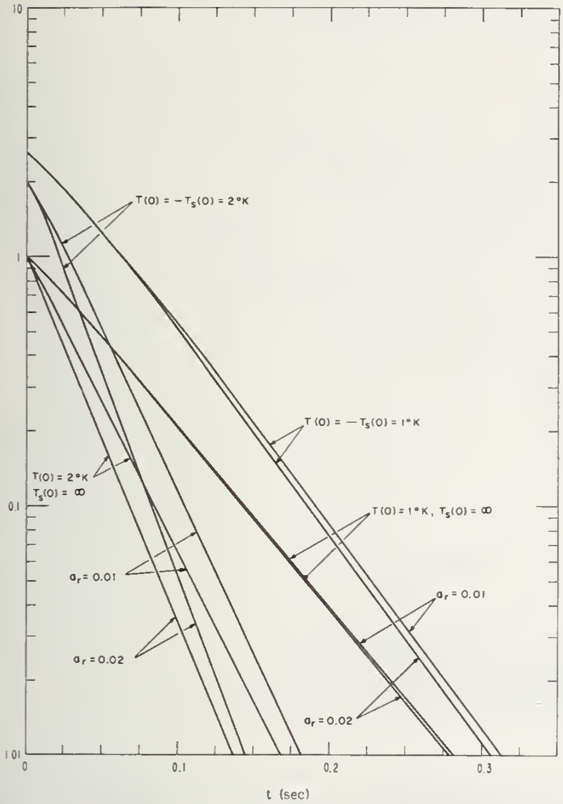

FIGURE 10. *Semi-log plot of transient magnetization after initial saturation and complete inversion.*

Resonant and remaining modes tightly coupled. $a_d = 10$ sec^{-1} deg^{-1}, $a_r = 0.01$ and 0.02 sec^{-1} deg^{-9}, $c_r = 1$ deg^5.

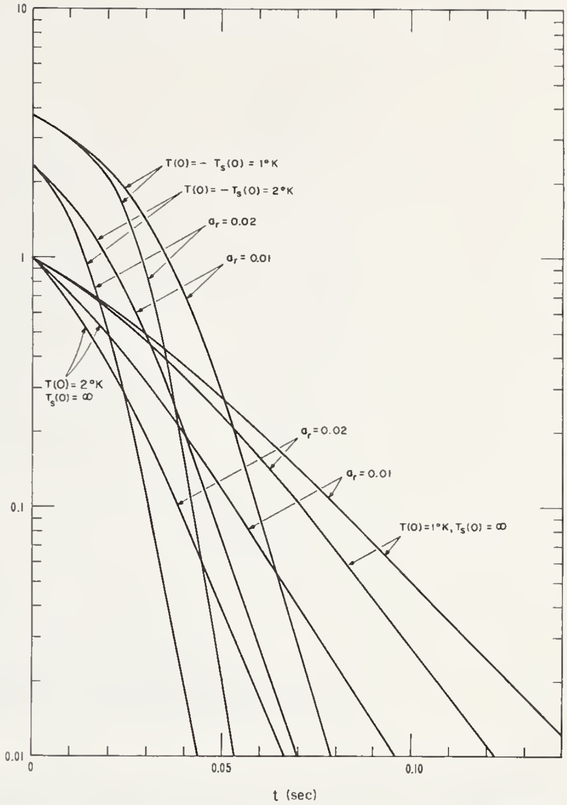

FIGURE 11. *Semi-log plot of transient magnetization after initial saturation and complete inversion.*

Resonant and remaining modes tightly coupled. $a_d = 10$ sec^{-1} deg^{-1}, $a_r = 0.01$ and 0.02 sec^{-1} deg^{-9}, $c_r = 10$ deg^5.

In obtaining eq (38d), we have used the fact that typically

$$\frac{c_d}{T_0^2} \gg 1, \frac{c_r}{T_0^5};$$

we have also assumed that τ_{d0} is of the order of, or less than τ_{r0}. Hence

$$\frac{d^2 s_0}{dt^2}\,(\text{inversion}) \gg \left|\frac{d^2 s_0}{dt^2}\right|\,(\text{saturation}).$$

Thus, at initial saturation, the spin relaxation rate begins at the initial direct-plus-Raman rate, but shortly falls to somewhat less than the Raman rate, when the resonant-phonon energy starts flowing back into the spin system. This rate then increases somewhat as the remaining lattice temperature rises. At initial inversion, the spin relaxation rate begins at twice that for saturation, and very rapidly increases until saturation is approached. This process will take place in a time shorter than the initial value of τ_d by a factor of the order of the ratio of T_0 to the maximum resonant-phonon temperature. This ratio can easily be 10^{-4} or less. The subsequent relaxation rate will be considerably slower than the Raman rate because of the extreme ease with which the energy of the very hot phonons flow back into the spin system. The spin system finds itself almost in a steady-state condition, with nearly constant magnetization. Eventually, the spin relaxation rate increases, both because the resonant phonons are cooler and the remaining lattice is warming up. The quantitative analysis which follows now will show that the slowing of the relaxation can be extremely pronounced, and would in fact be readily observable in an experiment for which the helium bath has been effectively removed, if there were no inelastic scattering of the phonons at the crystal boundaries. This kind of experiment could provide a measure of the degree of inelastic boundary scattering.

In figure 12, we assume initial spin saturation, with $T_d(0) = T_r(0) = 2$ °K, $a_d = 1$ sec^{-1} deg^{-1}, $a_r = 0.0043$ sec^{-1} deg^{-9}, $c_d = 10^5$ deg^2, and $c_r = 0.1$, 1, and 10 deg^5. The three curves may be compared with the appropriate spin saturation curves of figures 3 to 5. The first 100 msec of the latter is replotted in figure 12 as dashed curves. The first 20 msec of $s(t)$ and $T_d(t)$ is plotted on an expanded scale in the inset of figure 12. The inset shows clearly the slowing of the relaxation rate after about 3 msec, and the subsequent increase in the rate, particularly for the $c_r = 10$ deg^5 curve, due to the

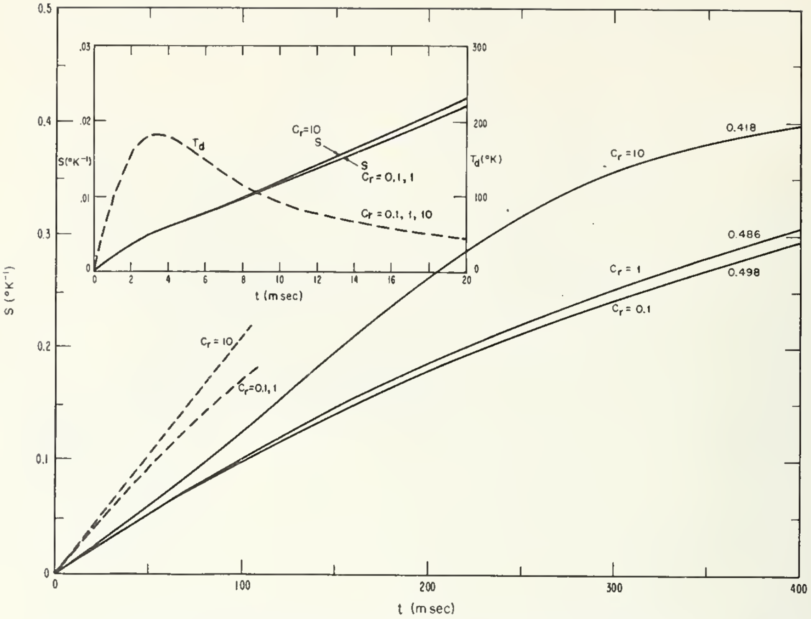

FIGURE 12. *Transient magnetization after spin saturation.*

Phonon modes uncoupled. $T_d(0) = T_r(0) = 2$ °K; $a_d = 1$ sec^{-1} deg^{-1}; $a_r = 0.0043$ sec^{-1} deg^{-9}; $c_d = 10^5$ deg^2 $c_r = 0.1$, 1, and 10 deg^5. The numbers 0.418, 0.486, and 0.498 are the asymptotic values of $s(t)$ in °K^{-1}. Dashe curves are taken from figures 3 to 5, and correspond to tightly coupled phonon modes. Inset: First 20 msec of magnetization and resonant-phonon temperature, on an expanded scale.

warming of the lattice. Overall, however, the relaxation is not very far from exponential, and an experiment using these parameter values, and saturation techniques, would likely not distinguish clearly between effectively coupled, and uncoupled, phonon modes.

In figure 13, initial spin inversion is assumed, all other conditions being the same as in figure 12. The initial rapid relaxation is plotted in the inset, which shows both $s(t)$ and $T_d(t)$. The near linearity between $s(t)$ and $T_d(t)$ during this initial period is a reflection of the near conservation of energy between the spin and resonant phonon systems. This is readily obtained from eqs (35) by setting a_r equal to zero, substituting eq (35b) into (35a), and integrating on time, giving

$$s(t) \approx s_0 + T_d(t)/c_d - T_0/c_d. \tag{39}$$

Equation (39) can also be used to estimate the maximum resonant phonon temperature, T_m, by setting $T_d(t) = [s(t)]^{-1} = T_m$. This gives, for an initial partial or complete spin inversion, and $c_d|s_0| \gg T_0$,

$$T_m \approx c_d|s_0| + T_0 + |s_0|^{-1} \approx c_d|s_0|. \tag{40a}$$

For near-saturation, which may be defined by the condition $|s_0c_d - T_0| \ll c_d^{1/2}$,

$$T_m \approx c_d^{1/2}. \tag{40b}$$

Since c_d is about 10^4 to 10^5 deg^2, the maximum resonant-phonon temperature can be more than two orders of magnitude greater after inversion than after saturation. This readily explains why the early saturation experiments designed to detect the hot phonons were unsuccessful, whereas the recent experiments using inversion techniques have succeeded [Brya and Wagner, 1965; Wagner and Brya, 1966; Shiren, 1966].

The three solid curves of figure 13 correspond to the left-hand scale. The right-hand scale corresponds to the dashed curve, which shows the relaxation behavior in its entirety for $c_r = 10$ deg^5. The $c_r = 0.1$ and 1 deg^5 curves are similar to this, but on a longer time scale. Of principal interest is the very flat region in the first 100 msec or so. The slope there is about 10^{-4} sec^{-1} deg^{-1}, whereas the slope due to a purely Raman relaxation in this region would be about $s_\infty/\tau_{r0} \approx (T_0\tau_{r0})^{-1} \approx 1$ sec^{-1} deg^{-1}.

Figures 14 and 15 are similar to figures 12 and 13, respectively, a_r being increased from 0.0043 to 0.01 sec^{-1} deg^{-9}, all other parameter values being unchanged. The features are qualitatively the same as in figures 12 and 13. In figure 14 (initial spin saturation), the resonant phonon temperature does not rise as high as in figure 12 for the reason that the higher Raman rate coefficient, a_r, allows a smaller proportion of the energy to flow into the resonant modes. The "halting" of the spin relaxation in figure 15 is as dramatic as in figure 13, although the spins are "released" somewhat earlier. Also, comparison of figures 13 and 15 shows that the initial rapid relaxation is quite insensitive to the Raman parameters a_r and c_r, as expected.

Figure 16 uses the same parameter values as figure 13, with the exception of c_d which is de-

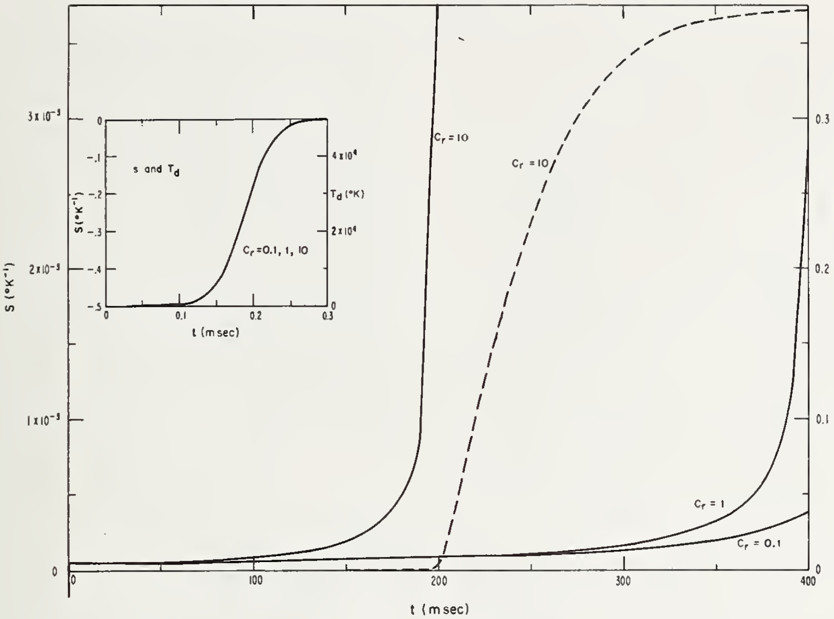

FIGURE 13. *Transient magnetization after complete spin inversion.*
Phonon modes uncoupled. Parameter values same as in figure 12. Left-hand scale for solid curves; right-hand scale for dashed curve. Inset: First 300 μsec of both $s(t)$ and $T_d(t)$ on an expanded time scale.

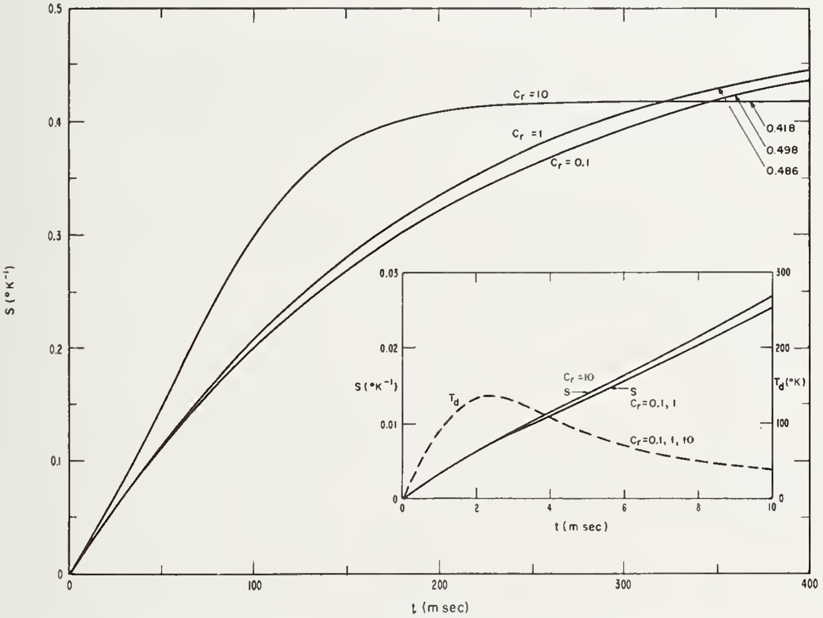

FIGURE 14. *Transient magnetization after initial spin saturation.*
Phonon modes uncoupled. $T_d(0)=T_r(0)=2$ °K; $a_d=1$ sec^{-1} deg^{-1}; $a_r=0.01$ sec^{-1} deg^{-9}; $c_d=10^5$ deg^2; $c_r=0.1$, 1, *and* 10 *deg*^{5}. The numbers 0.418. 0.486, and 0.498 are the asymptotic values of $s(t)$ in °K^{-1}. Inset: First 10 msec of $s(t)$ and $T_a(t)$ on an expanded scale.

creased from 10^5 to 5×10^4 deg^2. The only gross change is in the initial rapid relaxation from inversion to near-saturation. The initial relaxation now takes twice as long, and the resonant mode temperature rises only half as high as in figure 13. These results are in accord with expectations based on eq (40a). The subsequent slower relaxation is not quite as slow as in figure 13, the reason being that a smaller amount of energy is sent initially into the resonant modes.

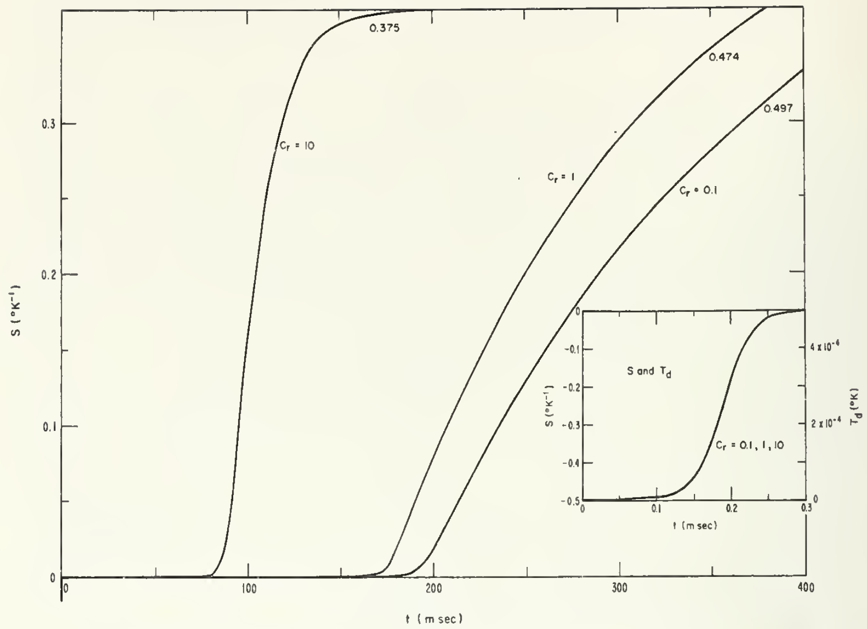

FIGURE 15. *Transient magnetization after complete spin inversion.*
Phonon modes uncoupled. Parameter values same as in figure 14. Inset: First 300 μsec of $s(t)$ and $T_d(t)$ on an expanded time scale.

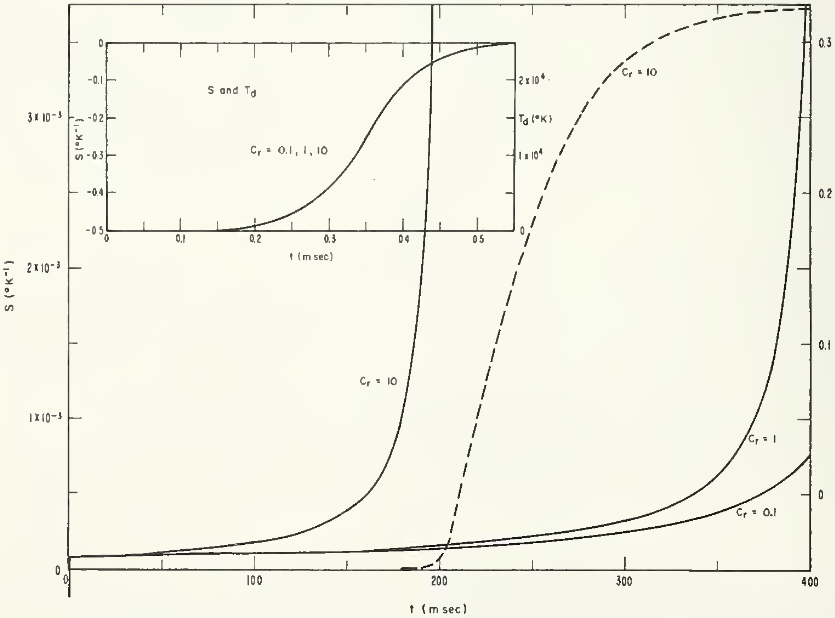

FIGURE 16. *Transient magnetization after complete spin inversion.*
Phonon modes uncoupled. $T_d(0)=T_r(0)=2$ °K; $a_d=1$ sec^{-1} deg^{-1}; $a_r=0.0043$ sec^{-1} deg^{-9}; $c_d=5\times 10^4$ deg^2 $c_r=0.1$, 1, and 10 deg^5. Left-hand scale for solid curves; right-hand scale for dashed curve. Inset: First half-msec of $s(t)$ and $T_d(t)$ on an expanded scale.

Figures 17 and 18 are analogous to figures 12 and 13, respectively, the difference being that in figures 17 and 18 we use $T_d(0)=T_r(0)=1$ °K rather than 2 °K. In figure 17, both $s(t)$ and $T_d(t)$ are plotted. Notice that the ordinate scale is different from that of figure 12. The most interesting feature of figure 17 is the initial "rapid" relaxation, a feature not so evident in figures 12 and 14. This "rapid" relaxation is of a different character than that resulting from an initial spin inversion, and is of course still described by eqs (38a, b). It is rapid only relative to the subsequent relaxation after about 10 msec, and in fact is only about half as fast as the initial relaxation of figure 12. After 10 msec, the relaxation proceeds somewhat slower than at the Raman rate, which is very small because of the low initial temperature, $T_r(0)=1$ °K.

Figure 18 may be compared with figure 13. The qualitative aspects are the same. The quantitative differences are the halved initial relaxation period and doubled maximum T_d over that of figure 13, as expected from eq (40a); and the much slower subsequent relaxation rate due to the lower T_0.

Figure 19 is analogous to figure 18, only c_d being changed, reduced to 5×10^4 deg^2 from 10^5 deg^2. Figure 19 may also be compared with figure 16, for which only the initial temperature is different.

In figures 20 and 21, we have changed a_d to 16 sec^{-1} deg^{-1}, and c_r to 0.4 deg^5, using $a_r=0.0043$ sec^{-1} deg^{-9} and $c_d=10^5$ deg^2 as in figures 12, 13, 17, and 18. These a_d and c_r values would obtain if the dc magnetic field, applied to a system for which $a_d=1$ sec^{-1} deg^{-1} and $c_r=0.1$ deg^5, were doubled. The $T_d(0)=T_r(0)=2$ °K curve of figure 20 may be compared with its equivalent in figure 12. An initial "rapid" relaxation now occurs, as a result of the faster direct relaxation rate. We have also plotted in figure 20, for $T_r(0)=2$ °K, curves for $T_d(0)=300$ °K, 10^3 °K, and 10^4 °K. These values can be considered to be the result of leaving the saturating microwave pulse on for various lengths of time. That is, while the microwave pulse is feeding energy into the spin system, the spin system is feeding energy into the vibrational modes. The resonant mode temperature will thus rise significantly if leakage of energy into the bath or into the remaining vibrational modes is sufficiently slow, as we are assuming in this section. The $T_d(0)=2$ °K curve would correspond to a short pulse, less than about 0.1 msec for the conditions of figure 20, as judged from the $T_d(t)$ curve of the inset, but intense enough to saturate the spin system. The effect of the longer pulses is to keep the relaxation from proceeding as far during the initial "rapid" phase. This effect, the decrease in amount of relaxation with increase in pulse length, is reminiscent of the results of Bowers and Mims [1959], and Bray et al. [1962] in saturation experiments. The *duration* of the initial decays they observed are of the same order as those in figure 20. However, the amount of decay in the initial relaxation in figure 20 constitutes only about 1 percent of the total amount [s(after rapid decay)/s(final) ≈ 0.01], whereas the corresponding figure in the Bowers and Mims, and Bray et al., experiments apparently can be of the order of 50 percent or more. Bowers and Mims [1959] have convincingly attributed their initial fast decays to

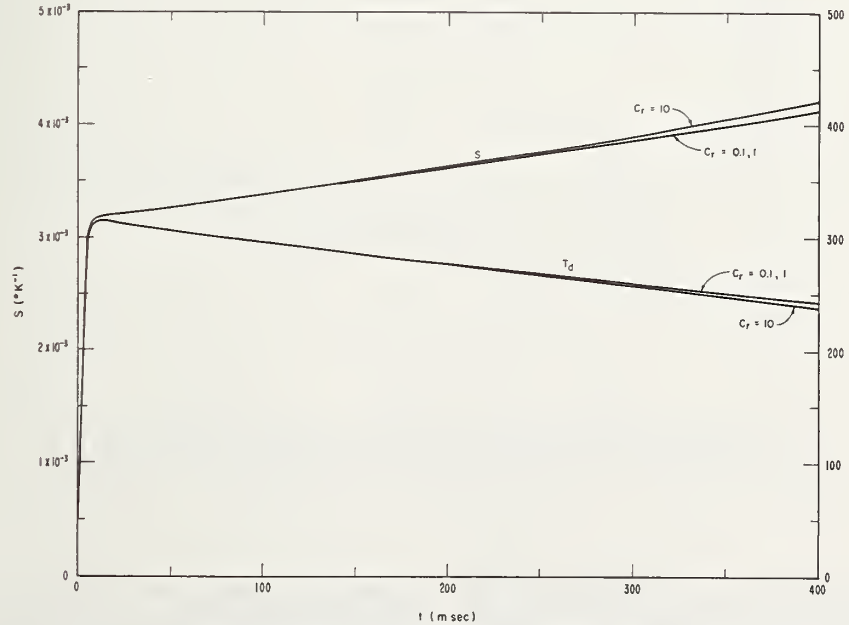

FIGURE 17. *Transient magnetization and resonant-phonon temperature after initial spin saturation.*

Phonon modes uncoupled. $T_d(0)=T_r(0)=1$ °K; $a_d=1$ sec^{-1} deg^{-1}; $a_r=0.0043$ sec^{-1} deg^{-1}; $c_d=10^5$ deg^2; $c_r=0.1$, 1, and 10 deg^5.

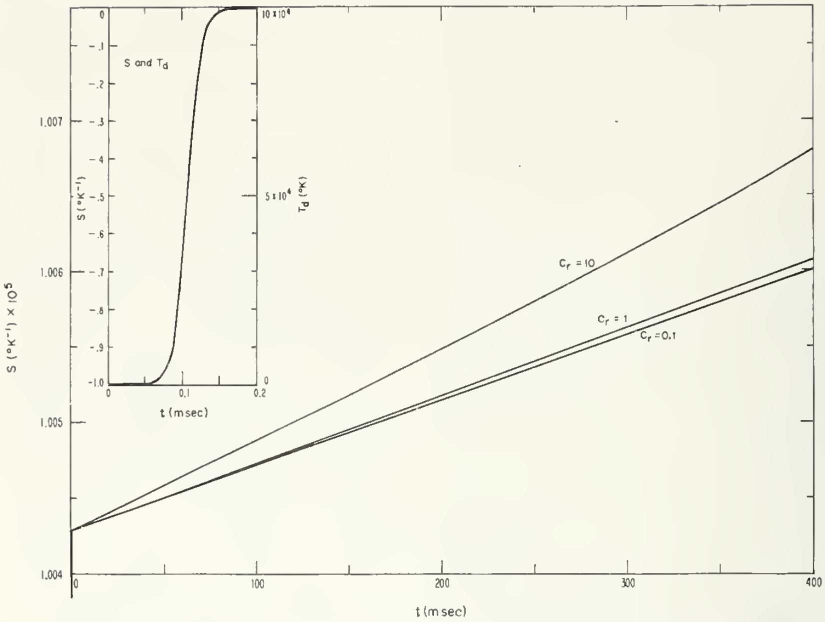

FIGURE 18. *Transient magnetization after complete spin inversion.*
Phonon modes uncoupled. Parameter values same as in figure 17. Inset: First 200 μsec of $s(t)$ and $T_d(t)$ on expanded time scale.

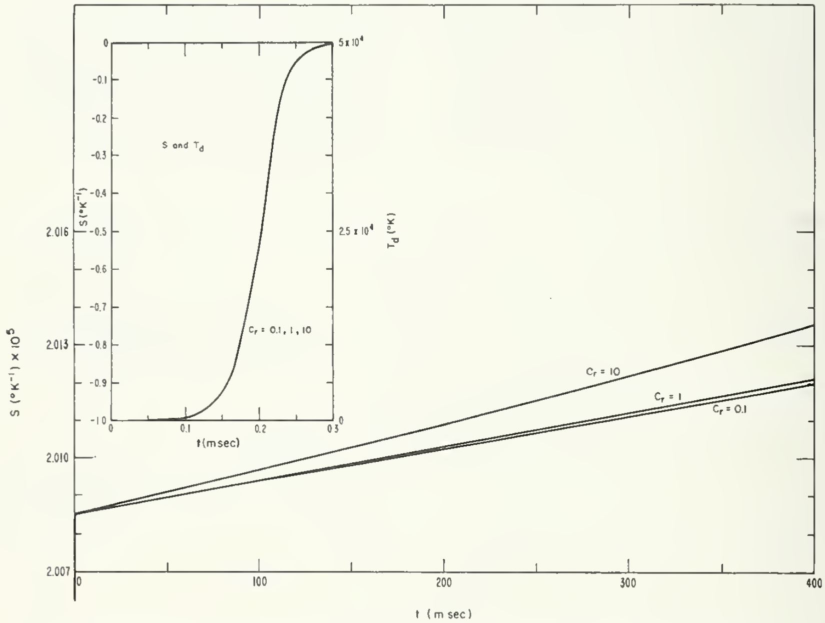

FIGURE 19. *Transient magnetization after complete spin inversion.*
Phonon modes uncoupled. $T_d(0)=T_r(0)=1$ °K; $a_d=1$ sec^{-1} deg^{-1}; $a_r=0.0043$ sec^{-1} deg^{-9}; $c_d=5\times 10^4$ deg^2; $c_r=0.1$, 1, and 10 deg^5. Inset: First 300 μsec of $s(t)$ and $T_d(t)$ on an expanded time scale.

spectral diffusion, that is to the sharing of the energy between those spins being pumped directly and those in other parts of their inhomogeneously broadened spin resonance line.

The slowing of the subsequent relaxation due to influx of energy from the resonant phonons is very evident in figure 20 for the higher $T_d(0)$ values. Notice that the highest value we use (10^4 °K) is still lower than the maximum resonant-phonon temperature which results from initial spin inversion. The curves of figure 20 can be thought of as indicating the transition from saturation to inversion.

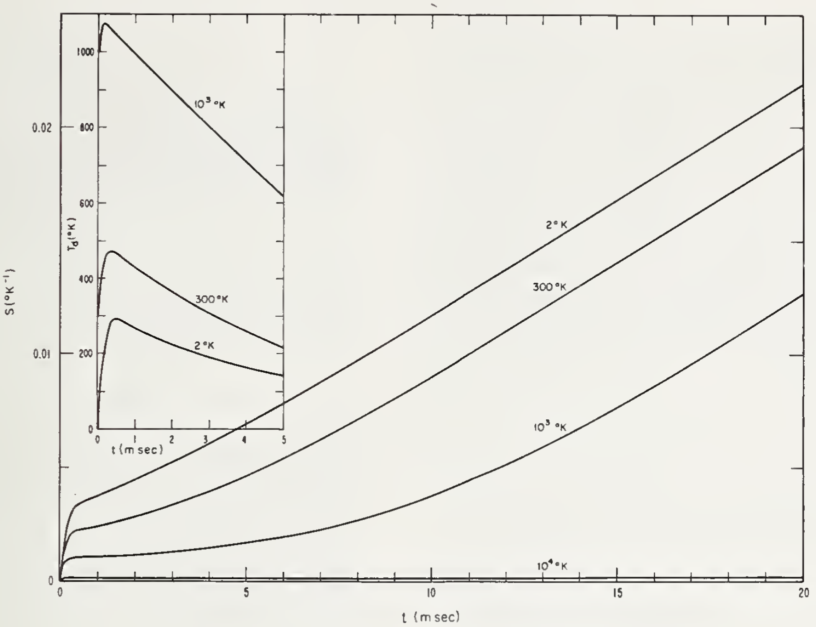

Figure 20. *Transient magnetization after spin saturation.*

Phonon modes uncoupled. $T_r(0) = 2$ °K; $T_d(0) = 2$ °K, 300 °K, 10^3 °K, and 10^4 °K; $a_d = 16$ sec^{-1} deg^{-1}; $a_r = 0.0043$ sec^{-1} deg^{-9}; $c_d = 10^5$ deg^2; $c_r = 0.4$ deg^5. Inset: First 5 msec of $T_d(t)$.

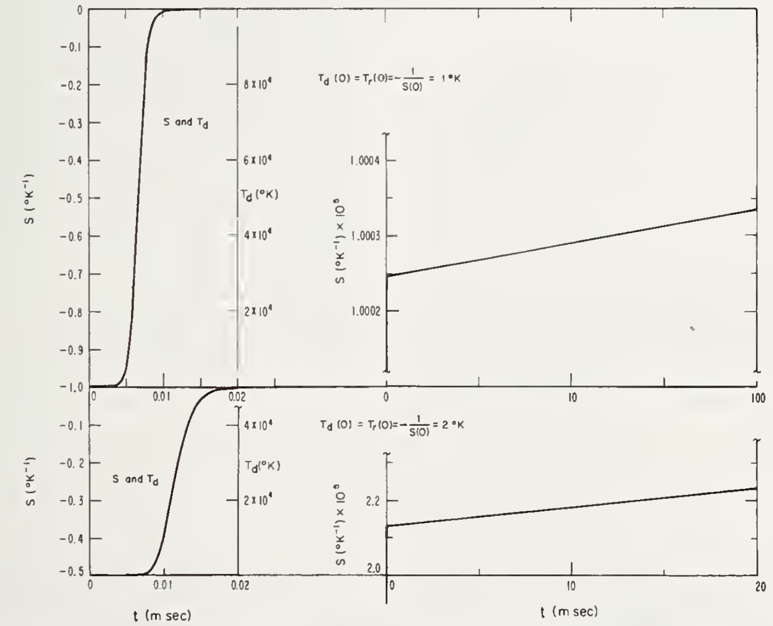

Figure 21. *Transient magnetization after complete spin inversion.*

Phonon modes uncoupled. Lower portion: $T_d(0) = T_r(0) = 2$ °K; upper portion: $T_d(0) = T_r(0) = 1$ °K. In both, $a_d = 16$ sec^{-1} deg^{-1}; $a_r = 0.0043$ sec^{-1} deg^{-9}; $c_d = 10^5$ deg^2; $c_r = 0.4$ deg^5.

The lower portion of figure 21 shows quantitatively the results of spin inversion from $T_d(0) = T_r(0) = 2$ °K, and the upper portion shows the results of spin inversion from $T_d(0) = T_r(0) = 1$ °K, for the same a_d, a_r, c_d, and c_r values as in figure 20. Notice that the initial rapid relaxation is now completed in 10–20 μsec.

As in the preceding section, the curves given in figures 12 to 21 apply to a broader range of relaxation times than explicitly used. That is, if a_d and

a_r are divided by the same factor f, the time scales of figures 12 to 21 may simply be multiplied by f to obtain the new curves.

In this section we have assumed that the resonant modes cannot communicate their energy to the remaining modes, and that energy cannot escape to a bath. The most significant result of these assumptions is the pronounced slowing of the spin relaxation after an initial period of rapid decay in which spin energy flows into the resonant mode system. This slow rate can be several orders of magnitude less than the Raman rate appropriate to the conditions used.

5. Spin Relaxation to the Resonant Phonons Coupled to a Bath

In the preceding two sections we investigated the transient spin behavior using the assumption that the usual bath had been removed, or could be ignored. The consequent heating of the resonant modes resulted in two dramatic effects: an initial rapid decay from spin inversion, and a subsequent very slow decay, slower than the Raman rate. The initial rapid decay has recently been seen by Brya and Wagner [1965, 1966].

In this section, we shall examine this latter effect in a little more detail. We assume that the spins are coupled only to the resonant phonons, which are in turn coupled to a bath at the constant temperature T_b, (Channels b, c, and e in fig. 1 are closed.) Spin coupling to the rest of the lattice will be neglected, because we are here interested chiefly in the behavior during the first few tens of microseconds. The Raman mechanisms, as we have seen, have very small influence during this interval. The bath may be helium surrounding the crystal, or it may be the rest of the lattice, if we assume that the temperature of this portion of the lattice does not change.

Equations (14) become

$$\frac{d\beta_s}{dt}=\frac{\beta_d-\beta_s}{\tau_d}, \tag{41a}$$

$$\frac{d\beta_d}{dt}=\frac{\beta_s-\beta_d}{\tau_d}R_{sd}+\frac{\beta_b-\beta_d}{\tau_b}, \tag{41b}$$

where τ_d and R_{sd} are given in eqs (32) and (36), respectively, and τ_b^{-1} is the instantaneous relaxation rate characterizing the rate of change of $\beta_d \equiv (kT_d)^{-1}$ due to the interaction between the resonant phonons and bath. In terms of $s(t)=k\beta_s$, $T_d(t)$, and T_b, eqs (41) are

$$ds/dt=a_d(1-sT_d), \tag{42a}$$

$$dT_d/dt=a_dc_d(1-sT_d)+(T_b-T_d)/\tau_{ph}, \tag{42b}$$

where

$$\tau_{ph}\equiv(T_b/T_d)\tau_b.$$

Now, the number of thermal phonons at the resonant energy Δ is given by the Planck factor, which is, in the high temperature approximation,

$$n=kT_d/\Delta.$$

Thus, by eq (42b), one can also write the rate of change of T_d due to the bath, in the form

$$\left.\frac{dn}{dt}\right|_{\text{bath}}=\frac{n_b-n}{\tau_{ph}} \tag{43}$$

where n_b is the number of thermal phonons at energy Δ at the final equilibrium temperature T_b. The usual assumption, and the one we adopt, is that the change of the phonon number due to interaction with the bath is a simple exponential process. Therefore τ_{ph} in eqs (43) and (42b) is taken to be independent of time.

If the bath is the surrounding helium, τ_{ph} is expected to be about $Q\ell/v$, where ℓ is the smallest dimension of the crystal, v is the average phonon speed, and Q is the number of boundary reflections before escape, which can be from one to about 100, depending upon surface condition and acoustic mismatch between crystal and helium. If the bath is the rest of the crystal, τ_{ph} would be characterized principally by inelastic boundary scattering [Faughnan and Strandberg, 1961; Scott and Jeffries, 1962]. A lower bound for this would be of the order of $\ell/v\approx 1$ μsec for a single crystal. Phonon-phonon times at liquid helium temperatures should be greater than milliseconds. Impurity scattering is elastic.

For finite values of τ_{ph}, eqs (42) have to be integrated numerically. For $\tau_{ph}=\infty$, however, the integration can be performed analytically to give

$$s(t)=2s_1+T_d(t)/c_d, \tag{44a}$$

$$T_d(t)=[s_2\coth(a_dc_ds_2t+\phi)+s_1]^{-1}, \tag{44b}$$

where

$$2s_1=s(0)-T_d(0)/c_d,$$

$$s_2=[s_1^2+c_d^{-1}]^{1/2},$$

$$\phi=\coth^{-1}\left(\frac{1-s_1T_d(0)}{s_2T_d(0)}\right).$$

Equations (44a, b) can be manipulated to give also

$$s(t)=s(0)+\frac{1-s(0)T_d(0)-s_1T_d(0)}{c_d[s(0)+s_2\coth(a_dc_ds_2t)]}. \tag{44c}$$

The magnetization and resonant-phonon temperature thus vary linearly with each other in the high temperature limit if $\tau_{ph}=\infty$.

In figures 22 to 25, we plot the quantity $-s(t)T_d(0)$ as a function of time for various values of c_d, using $\tau_{ph}=\infty$, 10 μsec, and 5 μsec, all with $a_d=100$ sec^{-1} deg^{-1}. The initial temperature $T_d(0)$ is always taken equal to the bath temperature T_b. Notice that complete inversion corresponds to a value of unity for the quantity $-s(0)T_d(0)$. We consider in each of figures 22 to 25, three degrees of initial inversion: 1, 0.60, and 0.25. We plot the transient behavior for only the initial relaxation to near-saturation; the subsequent relaxation to the bath is routine.

In figure 22, we use $T_d(0)=T_b=2$ °K and $c_d=2\times10^4$ deg^2. Most apparent is the increasing rapidity of relaxation with increasing degree of initial inversion. Notice that the influence of the bath is quite small for complete initial inversion, until saturation is nearly reached. This is true even for τ_{ph} as small as 5 μsec, although the initial relaxation takes about 12 μsec. The main effect of the bath is to flatten the curves somewhat before saturation is reached. The reason is that the phonons are being removed, thereby reducing the amount of stimulated relaxation of the spins.

Figure 23 uses the same parameter values as figure 22, except that $T_d(0)=T_b=1$ °K. The relaxation is seen to be somewhat faster in spite of the slower (halved) initial direct relaxation rate. The reason is that at lower temperatures, the ratio of spin to lattice heat capacity is increased (quadrupled in this case), thereby permitting a higher phonon temperature to be attained, with its consequent greater stimulation of spin relaxation. The experiments of Byra and Wagner [1965, 1966] were carried out at about 1.25 °K and 1.5 °K, on the cerium ion doped into lanthanum magnesium nitrate. The values of a_d and c_d used in figures 22 and 23 are approximately equal to the values appropriate to their experiments [Wagner and Brya, 1966]. Comparison of their results with figures 22 and 23 shows that the model used in this section has the features necessary to at least qualitatively describe the phonon avalanche. Brya and Wagner (private communication, preprint) have analyzed their results in some detail along lines similar to those used here, achieving at least qualitative agreement with the theory, although there are indications that the resonant-phonon mode bandwidth should be assumed to increase during the course of the relaxation.

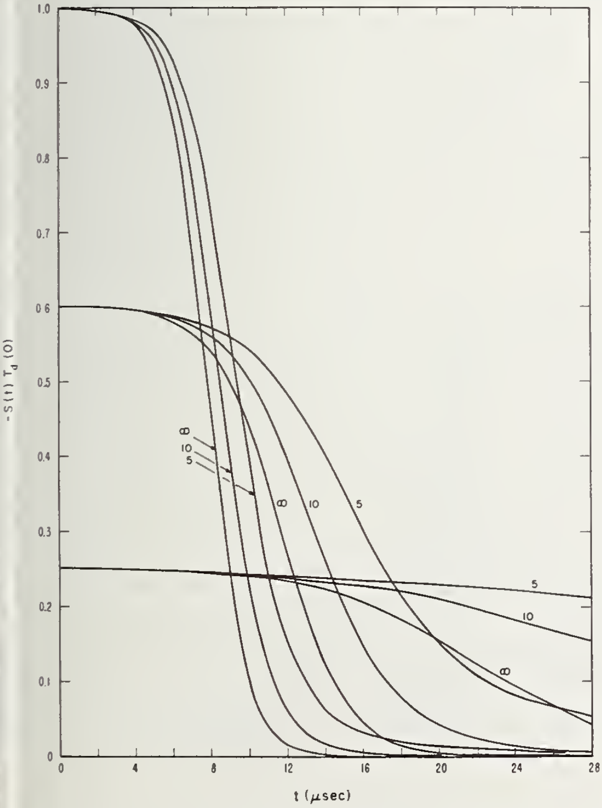

FIGURE 22. *Transient magnetization after three degrees of spin inversion: 1, 0.60, and 0.25.*

$Td(0)=T_b=2$ °K; $a_d=100$ sec^{-1} deg^{-1}; $c_d=2\times10^4$ deg^2. The numbers 5, 10, and ∞ are the values of τ_{ph} in μsec.

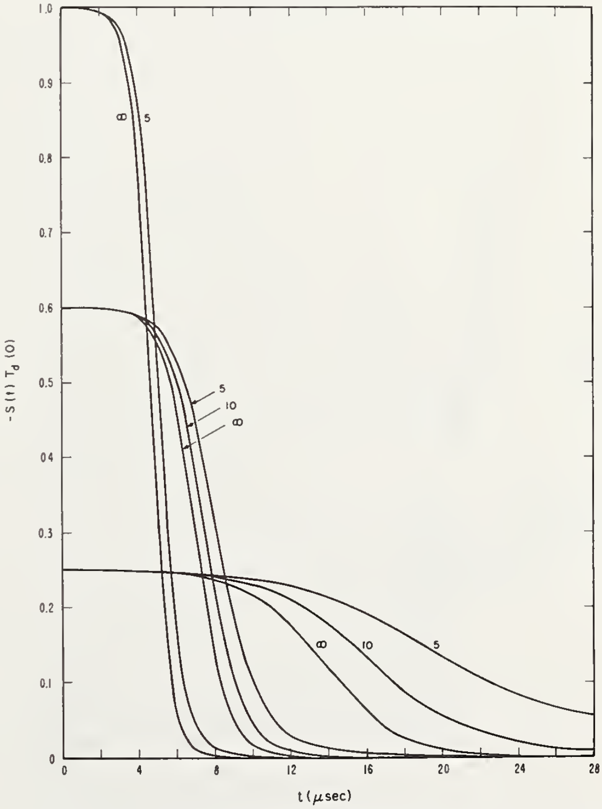

FIGURE 23. *Transient magnetization after three degrees of spin inversion: 1, 0.60, and 0.25.*

$T_d(0)=T_d=1$ °K; $a_d=100$ sec^{-1} deg^{-1}; $c_d=2\times10^4$ deg^2. The numbers 5, 10, and ∞ are the values of τ_{ph} in μsec.

In figure 24, we use $c_d = 5 \times 10^4$ deg^2, and in figure 25, we use $c_d = 10^5$ deg^2, both with $T_d(0) = T_b = 2$ °K. The relaxation is faster and the bath has less influence than in figure 22, as expected. Notice the changed time scale in figure 25.

As mentioned above, we have plotted in figures 22 to 25 only the phonon avalanche portion of the relaxation. One can readily show from eqs (42) that asymptotically the relaxation is exponential with a relaxation time given by

$$\tau = (\sigma + 1) T_d(0) + \text{terms of order } \tau_{ph}. \qquad (45)$$

Here σ is the "bottleneck factor," a parameter frequently used [Ruby et al., 1962; Wagner and Brya, 1966; Faughnan and Strandberg, 1961; Scott and Jeffries, 1962] in characterizing a material for which there is significant phonon heating. It is given by

$$\sigma = a_d c_d \tau_{ph} T_b^{-1}. \qquad (46)$$

When $\sigma \gg 1$, the asymptotic relaxation time is approximately proportional to T_b^{-2}, a temperature dependence characteristically seen in bottlenecked materials.

6. Discussion and Summary

In this article, we have presented the results of numerical computations of the transient magnetization of a paramagnetic substance, under conditions in which the lattice can heat up as the magnetic energy flows into it. Lattice heating can occur significantly at liquid helium temperatures if the bath is removed. If the lattice modes are effectively coupled to each other, which is likely to be the case if the time scale of the magnetic relaxation is of the order of 10^{-4} sec or larger, we have seen that deviation from exponential relaxation is not usually very large, although probably experimentally observable. The deviation is in the form of an increasing relaxation rate, due to the increasing lattice temperature.

If the so-called resonant-phonon modes are completely uncoupled from the remaining phonon modes (again with the bath removed), two dramatic effects can occur if the spins are initially inverted. First, there is a rapid decay to near-saturation, due to stimulated emission of resonant phonons, which by assumption are unable to escape from the crystal. The energy of these phonons has nowhere to go but back into the spin system, and does, as the spin

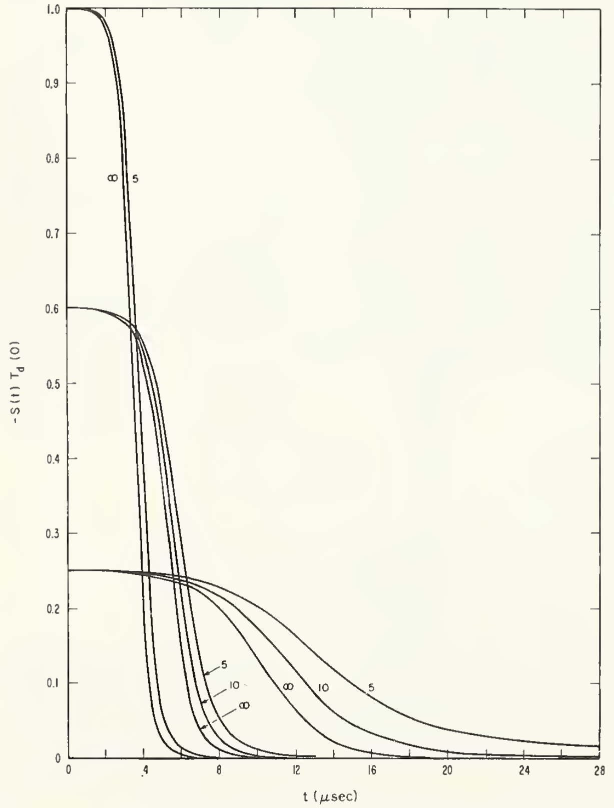

FIGURE 24. *Transient magnetization after three degrees of spin inversion: 1, 0.60, and 0.25.*

$T_d(0) = T_b = 2$ °K; $a_d = 100$ sec^{-1} deg^{-1}; $c_d = 5 \times 10^4$ deg^2. The numbers 5, 10, and ∞ are the values of τ_{ph} in μsec.

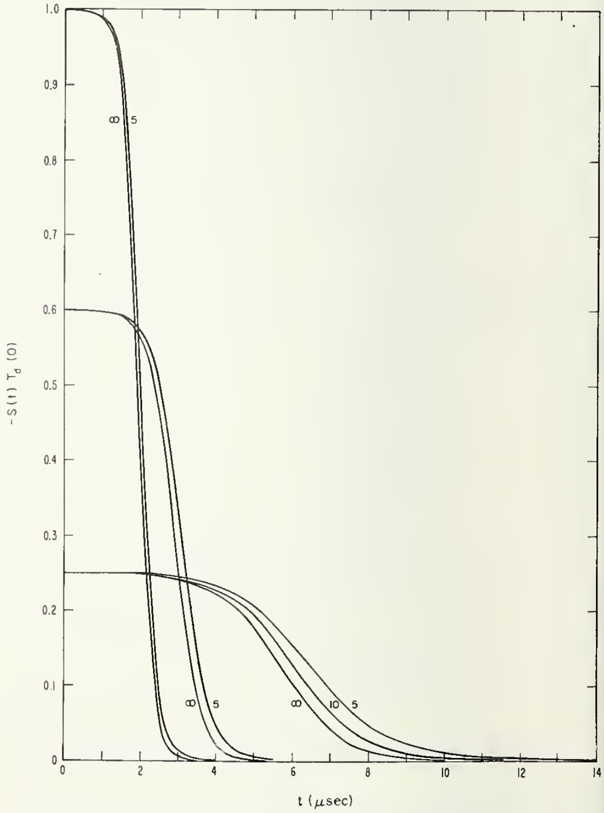

FIGURE 25. *Transient magnetization after three degrees of spin inversion: 1, 0.60, and 0.25.*

$T_d(0) = T_b = 2$ °K; $a_d = 100$ sec^{-1} deg^{-1}; $c_d = 10^5$ deg^2. The numbers 5, 10, and ∞ are the values of τ_{ph} in μsec.

system relaxes via a Raman process to the remaining modes. The result is that for a certain period, the energy content, and hence the magnetic moment, of the spin system is nearly stationary, which is the second effect mentioned above. Eventually the relaxation rate begins to increase, finally reaching the Raman rate appropriate to the final lattice temperature. This second effect, the severe suppression of the spin relaxation after the rapid decay, is expected to be difficult to observe even if the bath is effectively removed, because of the inevitable scattering of the phonons from grain boundaries. This scattering is partly inelastic, and thus partly short circuits the energy flow of the resonant phonons through the spin system. Phonon-phonon scattering conceivably could also be significant if the boundary scattering were very greatly reduced. Quantitative information on these two effects is usually not available. Ultrasonic attenuation measurements usually do not distinguish between phonon-phonon and phonon-boundary scattering. However, there is little doubt that the direct phonon-phonon relaxation times are greater than milliseconds at helium temperatures. Whether the use of a good single crystal with highly polished surfaces would suppress the inelastic scattering sufficiently to permit observation of the suppressed spin relaxation, remains to be discovered.

These considerations suggest, in fact, a possible new way of investigating the amount of inelastic boundary scattering of phonons as a function of frequency, temperature, crystal perfection, and surface condition, at microwave frequencies. That is, the spin signal may be monitored to determine the degree of suppression of relaxation. The latter, of course, can be calculated, as we have done in section 4, under the assumption of resonant-phonon decay only to the spin system.

However, it is likely that the results of such experiments would only confirm our expectation that boundary scattering is usually strong enough to mask the suppressed spin relaxation. The observations of Brya and Wagner [1965, 1966], the model for which is discussed in section 5, suggest another possible way of investigating boundary scattering, and perhaps also phonon-phonon scattering (which is temperature dependent [Faughnan and Strandberg, 1961; Herring, 1954]). Measurement of the spin decay, and hence the hot-phonon decay, after completion of the phonon avalanche, will provide information about boundary scattering as a function of the several parameters mentioned above. One might then attempt to see phonon-phonon effects by using a multi-mode cavity to create two successive avalanches at two neighboring frequency bands, and determining whether the decay rate in one band is influenced by the presence of the other.

I wish to thank Prof. P. E. Wagner for several discussions about his experiments, and Dr. J. S. Wells for his comments on experimental procedures. I also thank Miss Garney Hardy and Mr. Alfred Steele for their assistance with the numerical work.

7. References

Baker, J., B. Bleaney, and K. Bowers (1956), Paramagnetic resonance in some complex cyanides of the iron group, Proc. Phys. Soc. (London) **B69**, 1205.

Bowers, K. D., and W. B. Mims (1959), Paramagnetic relaxation in nickel fluosilicate, Phys. Rev. **115**, 285.

Bray, T., G. Brown, and A. Kiel (1962), Paramagnetic relaxation of Fe^{3+} in potassium cobalticyanide, Phys. Rev. **127**, 730.

Brya, W. J., and P. E. Wagner (1965), Paramagnetic relaxation to a bottlenecked lattice: development of the phonon avalanche, Phys. Rev. Letters **14**, 431.

Casimir, W. B. G. (1938), Note on the conduction of heat in crystals, Physica **5**, 495.

Casimir, W. B. G., and F. K. DuPre (1938), Note on the thermodynamic interpretation of paramagnetic relaxation phenomena, Physica **5**, 507.

Davids, D. A., and P. E. Wagner (1964), Magnetic field dependence of paramagnetic relaxation in a Kramers' salt, Phys. Rev. Letters **12**, 141.

Faughnan, B. W., and M. W. P. Strandberg (1961), The role of phonons in paramagnetic relaxation, J. Phys. Chem. Solids **19**, 155.

Gorter, C. J. (1947), *Paramagnetic Relaxation* (Elsevier Publishing Co. Inc., New York), pp. 89–90.

Hebel, L. C., Jr. (1963), in *Solid State Physics*, edited by F. Seitz and D. Turnbull (Academic Press, Inc., New York), Vol. 15, pp. 418–420.

Herring, C. (1954), Role of low-energy phonons in thermal conduction, Phys. Rev. **95**, 954.

Kronig, R. de L. (1939), On the mechanism of paramagnetic relaxation, Physica **6**, 33.

Orbach, R. (1961), Spin-lattice relaxation in rare-earth salts, Proc. Roy. Soc. **A264**, 458.

Paxman, D. (1961), Spin-lattice relaxation time measurements in dilute potassium ferricyanide, Proc. Phys. Soc. (London) **78**, 180.

Peterson, R. L. (1965a), Effects of finite lattice heat capacity on spin-lattice relaxation, Phys. Rev. **137**, A1444.

Peterson, R. L. (1965b), Theory of relaxation in a group of weakly coupled systems, Phys. Rev. **139**, A1151. This paper and [Peterson, 1965a] contain several earlier references giving the derivation and uses of the Pauli equation.

Philippot, J. (1964), Spin-spin relaxation and spin temperatures, Phys. Rev. **133**, A471.

Rannestad, A., and P. E. Wagner (1963), Paramagnetic relaxation in dilute potassium ferricyanide, Phys. Rev. **131**, 1953.

Ruby, R. H., H. Benoit, and C. D. Jeffries (1962), Paramagnetic resonance below 1 °K: spin-lattice relaxation of Cc^{3+} and Nd^{3+} in lanthanum magnesium nitrate, Phys. Rev. **127**, 51.

Scott, P. L., and C. D. Jeffries (1962), Spin-lattice relaxation in some rare-earth salts at helium temperatures; observation of the phonon bottleneck, Phys. Rev. **127**, 32.

Shiren, N. S. (1966), Observation of phonons generated in paramagnetic relaxation, Phys. Rev. Letters **17**, 958.

Van Vleck, J. H. (1940), Paramagnetic relaxation times for titanium and chrome alum, Phys. Rev. **57**, 426.

Van Vleck, J. H. (1941), Paramagnetic relaxation and the equilibrium of lattice oscillators, Phys. Rev. **59**, 724.

Wagner, P. E., and W. J. Brya (1966), in *Physics of Quantum Electronics*, edited by P. L. Kelley, B. Lax, and P. E. Tannenwald (McGraw-Hill, New York), "Stimulated phonon emission from an inverted spin system to a bottlenecked lattice," p. 376.

Ziman, J. M. (1960), *Electrons and Phonons* (Oxford University Press, London), Chap. XI.

U.S. GOVERNMENT PRINTING OFFICE : 1967 OL—261-405

NBS TECHNICAL PUBLICATIONS

PERIODICALS

- **JOURNAL OF RESEARCH** reports National Bureau of Standards research and development in physics, mathematics, chemistry, and engineering. Comprehensive scientific papers give complete details of the work, including laboratory data, experimental procedures, and theoretical and mathematical analyses. Illustrated with photographs, drawings, and charts.

Published in three sections, available separately:

- **Physics and Chemistry**

Papers of interest primarily to scientists working in these fields. This section covers a broad range of physical and chemical research, with major emphasis on standards of physical measurement, fundamental constants, and properties of matter. Issued six times a year. Annual subscription: Domestic, $5.00; foreign, $6.00*.

- **Mathematics and Mathematical Physics**

Studies and compilations designed mainly for the mathematician and theoretical physicist. Topics in mathematical statistics, theory of experiment design, numerical analysis, theoretical physics and chemistry, logical design and programming of computers and computer systems. Short numerical tables. Issued quarterly. Annual subscription: Domestic, $2.25; foreign, $2.75*.

- **Engineering and Instrumentation**

Reporting results of interest chiefly to the engineer and the applied scientist. This section includes many of the new developments in instrumentation resulting from the Bureau's work in physical measurement, data processing, and development of test methods. It will also cover some of the work in acoustics, applied mechanics, building research, and cryogenic engineering. Issued quarterly. Annual subscription: Domestic, $2.75; foreign, $3.50*.

- **TECHNICAL NEWS BULLETIN**

The best single source of information concerning the Bureau's research, developmental, cooperative and publication activities, this monthly publication is designed for the industry-oriented individual whose daily work involves intimate contact with science and technology—*for engineers, chemists, physicists, research managers, product-development managers, and company executives.* Annual subscription: Domestic, $1.50; foreign, $2.25*.

* Difference in price is due to extra cost of foreign mailing.

NONPERIODICALS

Applied Mathematics Series. Mathematical tables, manuals, and studies.

Building Science Series. Research results, test methods, and performance criteria of building materials, components, systems, and structures.

Handbooks. Recommended codes of engineering and industrial practice (including safety codes) developed in cooperation with interested industries, professional organizations, and regulatory bodies.

Miscellaneous Publications. Charts, administrative pamphlets, Annual reports of the Bureau, conference reports, bibliographies, etc.

Monographs. Major contributions to the technical literature on various subjects related to the Bureau's scientific and technical activities.

National Standard Reference Data Series. NSRDS provides quantitative data on the physical and chemical properties of materials, compiled from the world's literature and critically evaluated.

Product Standards. Provide requirements for sizes, types, quality and methods for testing various industrial products. These standards are developed cooperatively with interested Government and industry groups and provide the basis for common understanding of product characteristics for both buyers and sellers. Their use is voluntary.

Technical Notes. This series consists of communications and reports (covering both other agency and NBS-sponsored work) of limited or transitory interest.

CLEARINGHOUSE

The Clearinghouse for Federal Scientific and Technical Information, operated by NBS, supplies unclassified information related to Government-generated science and technology in defense, space, atomic energy, and other national programs. For further information on Clearinghouse services, write: Clearinghouse

U.S. Department of Commerce
Springfield, Virginia 22151

Order NBS publications from:

Superintendent of Documents
Government Printing Office
Washington, D.C. 20402

U.S. DEPARTMENT OF COMMERCE
WASHINGTON, D.C. 20230

OFFICIAL BUSINESS

POSTAGE AND FEES PAID
U.S. DEPARTMENT OF COMMERCE